Phase Behavior and Microemulsion Studies On a Saudi Arabian Crude

by

Alhasan B. Fuseni

A Thesis Presented to the

FACULTY OF THE COLLEGE OF GRADUATE STUDIES

KING FAHD UNIVERSITY OF PETROLEUM & MINERALS

DHAHRAN, SAUDI ARABIA

In Partial Fulfillment of the
Requirements for the Degree of

MASTER OF SCIENCE

In

PETROLEUM ENGIEERING

July, 1987

Order Number 1355745

Phase behavior and microemulsion studies on a Saudi Arabian crude

Fuseni, Alhasan B., M.S.

King Fahd University of Petroleum and Minerals (Saudi Arabia), 1987

U·M·I
300 N. Zeeb Rd.
Ann Arbor, MI 48106

PHASE BEHAVIOR AND MICROEMULSION STUDIES ON A SAUDI ARABIAN CRUDE

BY

ALHASAN B. FUSENI

A Thesis Presented to the
FACULTY OF THE COLLEGE OF GRADUATE STUDIES
KING FAHD
UNIVERSITY OF PETROLEUM & MINERALS
DHAHRAN, SAUDI ARABIA

In Partial Fulfillment of the
Requirements for the Degree of

MASTER OF SCIENCE
IN
PETROLEUM ENGINEERING

JULY 1987

PRINTED BY: UPM PRESS

King Fahd UNIVERSITY OF PETROLEUM & MINERALS

DHAHRAN, SAUDI ARABIA

This thesis, written by *Mr. Alhasan Bin Fuseni* under the direction of his thesis committee, and approved by all the members, has been presented to and accepted by the Dean, College of Graduate Studies, in partial fulfillment of the requirements for the degree of MASTER OF SCIENCE IN PETROLEUM ENGINEERING

Dr. Abdullah S. Al-Zakri
Dean, College of Graduate Studies

Date : July 4, 1987

Dr. Muhammad A. Al-Marhoun
Department Chairman

Thesis Committee

Dr. Mehmet S. Celik, Chairman

Dr. Sidqi A. Abu-Khamsin, Member

Dr. Habib Menouar, Member

Dedicated to my parents.

ACKNOWLEDGMENTS

Praise and thanks to Allah for making this thesis a reality.

Acknowledgment is due to the King Fahd University of Petroleum and Minerals for the opportunity to produce this thesis and especially to Dr. Muhammed A. Al-Marhoun, Chairman, Petroleum Engineering Department for the great understanding and support during my stay in the University.

I am also greatly indebted to my thesis committee chiarman, Dr. Mehmet S. Celik for his carefull supervision and ever-ready help that made the early completion of this work possible. His motivation, encouragment and work over the weekends are greatfully acknowledged. I deeply appreciate the guidance and suggestions provided by the other members of the thesis committee, Dr. Sidqi Abu-Khamsin and Dr. Habib Menouar.

I wish to express my thanks to the Petroleum Engineering Section, Petroleum and Gas Engineering Division , KFUPM Research Institute, for providing facilities for Interfacial Tension and Viscosity measurements.

Thanks are also due to the members of the Surfactant/Polymer Flooding research group (KACST project No.AR-6-161) for their support. Finally, I would like to thank the KACST for providing the financial assistance.

TABLE OF CONTENTS

LIST OF TABLES

LIST OF FIGURES

NOMENCLATURE

A	= alcohol
ACN	= alkane carbon number
C	= overall composition
C_o	= concentration of surfactant in oil (g/l)
C_d	= drop shape constant
C_w	= concentration of surfactant in brine (g/l)
EACN	= equivalent alkane carbon number
EO	= ethoxylation number
HTAB	= hexadeycltrimethylammoniumbromide
IFT	= interfacial tension (dynes/cm)
k	= constant ascribed to surfactant type
l	= chainlength
M	= molarity (moles/l)
MEAC12OXS	= monoethanol amine salt of dodecylorthoxylene sulfonic acid
NaCl	= sodium chloride
N_{min}	= constant ascribed surfactant chainlength
O/W	= oil-in-water microemulsion
p	= period of rotation (ms/rev)
PIT	= phase inversion temperature
rpm	= revolution per minute
S	= % sodium chloride concentration

TAA	= tertiary amyl alcohol
W/O	= water-in-oil microemulsion
WOR	= water-oil ratio

Greek Letters

α	= critical exponent describing specific heat
γ	= interfacial tension (dynes/cm)
π	= pi (3.142)
σ	= solubilization parameter
ν	= critical exponent describing divergence of correlation length
Δ	= difference
ρ	= density (g/cc)
ω	= angular velocity (rad/s)

Subscripts

a	= alcohol
AM	= between aqueous and microemulsion phases
AO	= between aqueous and oleic phases
MW	= between microemulsion and brine phases
o	= oil
OM	= between oleic and microemulsion phases
s	= surfactant
w	= brine

ملخـــص

ان معرفة السلوك الطورى لكتلة المزيح خلال تقدمها فى حالاتها المختلفه لمن العوامل المهمه للمحافظة على ازاحة فعالة للزيت با ستخدام الازاحـــــه الجزئية . ولقد اوضحت تجارب الغمر للعينات اللبية أن كميات معتبرة مـــــن الزيت تتبقي عندما تتحطم الكتلة الى اطوار مختلفة . ويمكن ازاحة معظـــــم الزيت المتبقي اذا تم تقليل التوتر البيني بين الاطوار الى أدني حد .

ولهذا لقد تمت دراسة السلوك الطورى للكتلة المتعددة الاطوار فـــــى ظروف مماثلة للتى فى الممكن (درجة حرارة تساوى ٩٠ درجة مئوية وملوحـــــة تساوى ٢٠ ٪) . ولقد شملت الدراسة قياس التوتر البينى ومعامل التجـــــزؤ كما استخدمت نتائج الدراسة فى تحديد قيم الملوحة المثالية وايضا تم تمثيـــل الاطوار فى الرسم الثلاثى للاطوار .

ولقد اظهرت الدراسة شيئا ذا أهمية بالغة بالنسبة للملوحة والحـــرارة العاليتين الموجودتين فى مكامن الصخور العربية السعودية الا وهو الملوحـــة المثالية الثانوية التى تحدث عند ملوحة اعلى من الملوحة المثاليه الابتدائية (يعرف سابقا بالملوحة المثالية فقط) . وقد تم فحص وجود الملوحة المثاليـــة الثانوية لعينات من سلفونات واثوكسيليتية لها ارقام اثوكسيلية مختلفـــــة بوجود الزيت الخام والقلوى . فمثلا ، عند درجة حرارة تساوى ٩٠ درجة مئوية ورقم اثوكسيليتى يساوى ٨ وجد الملوحه المثالية الابتدائية عند ملوحة تساوى ٨٪

بينما وجد الملوحه المثالية الثانويةعند ملوحة تساوى ١٤ ٪ . ولقد لوحظ انه كلما ارتفع الرقم الهاثوكسيليتى كلما ارتفعت مستويات الملوحه التى تحدث عندها الملوحة المثالية الابتدائية والثانوية . واظهرت ايضا ان الملوحة المثالية الثانوية تنتج اقل توّثر بينى .

ان التمثيل الثلاثى لسلفونات الاثوكسيليتية ب ١٠٨٣ برقم اثوكسيليتى يساوى ١٥ ، اظهر ان الملوحة التى تساوى ٢٠ ٪ والتى تقابل الملوحة المثالية الثانوية ينتج عنها مثلث طورى جيد وفعال للازاحة . والاهم من ذلك انه فى منطقة الاطوار الثلاثة التى يختلف عندها نسب الماء الى الزيت . وان هذه الظاهرة تساعد فى تخمين او التنبوّ بالسلوك الطورى فى ظروف مماثلة للتى فى الممكن .

ABSTRACT

The knowledge of phase behavior of the slug as it proceeds through different stages is an important factor to maintain an efficient displacement of oil in micellar flooding systems. Coreflood experiments have shown that a considerable amount of oil is left behind when a slug breaks down into several phases. The amount of oil left by the slug may be drastically reduced if the interfacial tensions (IFT's) between the phases are kept as low as possible. In this regard, the phase behavior of the multiphase slug has been studied under relevant reservoir conditions of 20% salinity and 90°C of temperature for properties including interfacial tension and partition coefficients. Based on the above data optimal salinities were determined and pseudoternary diagrams constructed.

A new finding of crucial importance to high-salinity and high-temperature Saudi Arabian Limestone reservoirs is presented. The existence of a secondary optimal salinity which occurs at salinities higher than the primary optimal salinity (previously known as optimal salinity) has been revealed by this study. The presence of a secondary optimal salinity has been tested for ethoxylated sulfonates of varying ethoxylation number with an alkane and a crude oil. For example, for EO=8 while the primary optimal salinity at 90°C takes place at 8% salinity, the secondary optimal salinity occurs at 14% salinity.

Increasing the EO number shifts the primary and secondary optimal salinties to higher salinity levels further confirming the reality of this finding. Moreover, the data show that the secondary optimal salinity yields even lower interfacial tensions.

Ternary representations with the ethoxylated sulfonate B1083, EO=15 revealed that 20% salinity which corresponds to the secondary optimal salinity, produced a symmetric three phase "triangle". This implies that the salinity level of 20% gives good IFT lowering and efficient displacement. More importantly, for the target conditions of salinity and temperature, the solutions remain in the three phase region- the lowest IFT region- with widely varying water to oil ratios. This feature can facilitate the prediction of the phase behavior under actual field conditions.

CHAPTER 1

CHAPTER 1

INTRODUCTION

Surfactant/polymer flooding offers a potential opportunity for Saudi Arabia, as over 50% of residual oil may remain in wateflooded Saudi Arabian oil fields. Since Saudi Arabian crude oils are predominantly low to medium viscosity, this process can provide a suitable means to improve the final recovery.

Entrapment of oil in the reservoir occurs because the oil droplets are not deformable enough to allow the available pressure gradient to push them through the pore throats. This condition occurs after the reservoir had used up its natural drive and also after waterflooding. At this condition the interfacial tension (IFT) between the oil droplets and reservoir brine is rather high, between 20 and 30 dynes/cm, which approximately corresponds to a capillary number of 10^{-7}.

Surfactant/polymer flooding is a multi-slug process involving sequential injection of surfactant solution, polymer solution and drive water. Mobilization of the trapped oil is achieved through selected surfactants which are capable of reducing interfacial tension at the water/oil interface to about 10^{-3} dynes/cm. At the interfaces, the mixture of injected chemicals and reservoir fluids, namely brine, surfactant and oil, may form a microemulsion. The mixture produced is

then pushed through the reservoir by a mobility control agent, polymer, followed by chase water. The displaced oil ganglia form an oil bank that is progressively pushed towards the production well.

In surfactant flooding, the formation of microemulsion results when water, oil and surfactant and/or cosurfactant equilibrate at surfactant concentrations in excess of the critical micelle concentration (CMC). This observation reveals that all surfactant flooding processes will inevitably involve the formation of microemulsion. The microemulsions that are formed will reduce interfacial tension and displace oil completely in the initial stages of the flooding process. However, the single phase microemulsion soon breaks down due to a multiplicity of factors. Among the factors are dispersion, adsorption and dilution both at the front and rear of the slug. Once the slug breaks down, three distinct phases appear, and the displacement process is no more miscible but immiscible.

After the formation of the three phases namely, oil, microemulsion and brine, displacement efficiency can still be maintained as long as the interfacial tension between oil and microemulsion and also between microemulsion and brine is kept very low. It was therefore the objective of this study to investigate the phase behavior of microemulsions using a Saudi crude oil and pure alkanes with the aim of formulating a microemulsion slug that will provide a high recovery efficiency. Phase behavior of the multiphase slug has been studied

under relevant reservoir conditions for phenomena including interfacial tension, partition coefficients and solubilization parameters. Based on the above data optimal salinities are determined and pseudo-ternary diagrams constructed to delineate the single and multiphase regions. The overall results are analyzed to formulate conditions that will achieve an effective microemulsion slug.

In addition, a new finding of crucial importance to high-salinity Saudi Arabian limestone reserviors is presented. This major finding "Existence of a Secondary Optimal Salinity" is expected to open new avenues in the design of new surfactant formulations in hostile environments, viz. Saudi Arabian limestone reserviors.

CHAPTER 2

CHAPTER 2

LITERATURE SURVEY

Since the first description of microemulsions by Schulman (1) there has been a large volume of publications on the subject of phase behavior. In general, they may be classified into two main groups. The first group consists of those that describe the phase behavior in surfactant flooding through experimental techniques. On the other hand, the second group describes phase behavior using mathematical models.

(i) Among the experimental investigators of phase behavior are Healy and Reed (3-4). In their first publication, they explored the physicochemical aspects of microemulsion flooding using a heavy aromatic naphtha. The characteristics of the multiphase region formed by an anionic surfactant were studied. The different phases were also mapped on ternary diagrams, and found to be consistent with Winsor's (2) conception. In a later publication (4), they concentrated on the multiphase region formed by a mixture of aromatic naptha and a paraffin with an anionic surfactant. This led to a correlation between interfacial tension and phase behavior, providing a basis for surfactant screening in micellar flooding systems. More importantly, they introduced a new concept, "optimal salinity", which has become the most important criterion for structuring surfactants to maximize solubilization of oil and

water.

Hsieh (6) in a Ph.D. dissertation studied the phase behavior of a pure oil with a petroleum sulfonate and found that alcohol type and concentration in a surfactant slug affects solubilization ability and hence its optimal salinity. The optimal salinity was observed to increase with the chain length of the alkanes. In close agreement with Hsieh's work, Shah (8) examined the fundamental aspects of microemulsion flooding in which a general overview including surfactant screening, the effects of oil chain length, salinity and electrolyte concentrations was given.

Bellocq et. al (16) explained the mechanisms responsible for low IFT using an anionic surfactant and a pure hydrocarbon. One of the mechanisms is the critical behavior of the microemulsion in the three phase region. In the two phase region low IFT was ascribed to the presence of a particular composition of the interfacial film between phases. It was also shown that, in ternary representation, the composition of the middle phase was a locus instead of a point.

The phase behavior of the monoethanol amine salt of dodecylorthoxylene sulfonic acid MEAC12OXS with a mixture of Isopar M, a paraffinic oil, and a heavy aromatic naphtha was studied by Glover et al (21). They showed that divalent ions react with surfactant to form insoluble divalent sulfonates which decrease the optimal salinity for the system under consideration. The reduction of optimal salinity was attributed to the negative contribution of divalent calcium sulfonate

species to optimal salinity.

Winsor (2) made the first phase behavior representations in micellar flooding and showed the different phase regions that result after equilibriating certain surfactant formulations. For low salinities, the phase behavior was described by Type I (see Fig. 4). This regime is characterized by a two phase region with negative tie line slopes such that any composition in this region will seperate into surfactant rich aqueous phase and oleic phase devoid of surfactant. At intermediate salinities the phase behavior was described by Type III. Any composition within the triangle equilibriates into three phases: microemulsion, excess water and excess oil. Further increase in salinity results in the Type II regime. The Type II diagram has a two phase region with positive tie line slopes such that any point in this region exhibits a surfactant rich oil phase and aqueous phase with almost no surfactant.

After the pioneering work of Winsor (2), Pope and Nelson (27) made extensive studies into representation of phase behavior in surfactant flooding. Among the interesting results that emerged from their work was the observation that equilibrium phases found in test tubes are representative of the phases produced in core flood experiments. Consequently, many performance characteristics of chemical floods could be explained and predicted from equilibrium surfactant-brine-oil phase diagrams. It was concluded that an oil reservoir under chemical

flooding could be visualized as a series of connected cells with phase equilibrium attained in each. They also emphasized that the surfactant slug should be designed to keep as much surfactant as possible for a prolonged period in the type III phase environment.

In his Ph.D dissertation, Salager (30) expounded more on ternary representation in micellar flooding. In particular he illustrated the location of the "bottom tie line". If significant amounts of surfactant partition into the oleic and aqueous phases in the type III region, a bottom tie line could be mapped to show the existence of a two phase region directly below the three phase triangle.

In order to use the concept of Winsor ternary diagram it is necessary to group several components at the same vertex since in practical cases the number of chemicals is larger than three. This gives rise to the so-called pseudoternary diagram where the pseudocomponents are assumed to behave as single pure components. In this representation the aqueous phase is generally a sodium chloride solution which simulates reservoir connate water, with salinity expressed as a percentage by weight. The oleic phase can range from a pure hydrocarbon to an extremely complex mixture such as a crude oil.

The concept of Equivalent Alkane Carbon Number (EACN) introduced by Cayais et. al (28), is a simple tool to approximate the phase behavior of a crude oil by a single pure alkane. The utilization

of pure alkanes simplifies considerably the analysis of experimental phenomena. One of the main problems in pseudoternary representation is to decide where to place the alcohol used as a co-surfactant. Previously, Healy and Reed (4) and Shah (8) used a fixed surfactant/alcohol ratio and considered it as a pseudocomponent assuming that each partitions in the same ratio. A large number of data reported by Salager (30) negates the above assumption. Also it was shown that alcohols which are not completely soluble in water are able to drastically modify phase behavior in a manner which contradicts Winsor's type III diagram concept.

From this discussion it seems that a reasonable approximation of a ternary diagram cannot be obtained for a multicomponent system. While it may not be possible to accurately construct the phase boundaries, it is possible to define the type of the diagram and to estimate most of its characteristics provided the following hold:

(1) The water vertex represents an aqueous sodium chloride solution.

(2) The oil vertex represents an alkane or a hydrocarbon phase in general.

(3) The surfactant vertex includes a surfactant or surfactant mixture but excludes alcohol.

A ternary diagram thus obtained will achieve its purpose of aiding the miceller flood designer to interpret the transitions from types I - III - II as defined by Winsor.

In a more recent publication the role of tricritical points in miceller flooding was emphasized by Smith (24). The achievement of ultralow interfacial tension was related to a critical point where the compositions of the phases concerned tend to approach each other. Experimental proof and theoretical discussion of this were first introduced by Fleming and Vinatieri (26). It was therefore explained that the primary function of surfactants in miceller flooding, is the creation of critical points, or at least near-critical conditions, in oil reservoirs. The widely held notion of surface active effects such as the formation of micelles, are of secondary importance.

Since it is almost impossible to create and maintain a composition in a reservoir and under flowing condition at a single critical point, the creation of coexisting critical solutions is sought. Achievement of three phases implies that there are three pairs of phases that must be simultaneously near the critical point.

A relatively new idea in miceller flood design is the salinity requirement diagram introduced by Nelson (18). The optimal salinity of a slug is the level of brine concentration at which oil displacement is most efficient. This optimal salinity and the range over which the slug is type III are dependent on the surfactant concentration. Because the surfactant concentration decreases as the flood proceeds due to dispersion and adsorption, the optimal salinity is bound to change also. A salinity requirement diagram expresses quantitatively the dependence

of midpoint salinity and the type III range on surfactant concentration.

Nelson (13) investigated the effect of pressure on phase behavior in surfactant flooding and found no appreciable effect. However, the phase behavior was affected when a lower molar-volume synthetic oil was substituted for stock tank oil. In contrast to this, Rossen and Kohn (15) revealed a significant effect of pressure on the phase behavior of their system. They, however, conceded that recent reports on the effect of pressure have not all been unanimous.

While most of the experimental work on micellar flood design has been done with anionic surfactants, nonionic surfactants have also received attention due to their insensitivity to harsh reservoir brines. Koukuonis et. al (14) examined the partitioning of ionic/nonionic mixtures. Their work revealed that the ionics partition differently from the nonionics and therefore the mixture cannot be assumed as a pseudo-component in ternary representation. Nonionic surfactants, ethoxylated nonylphenols, were investigated by Gracia et al (19), using pure alkanes at 28°C. While acknowledging that most commercial nonionic surfactants yield high IFT, low solubilization and medium temperature limit, they hold the conviction that new nonionics can be tailored to overcome the present shortcomings. It was shown that with proper design nonionics can favorably compare with anionics. They proposed that such new surfactants should be the ethyoxylated phenols with increased hydrophobe molecular weight and chainlength, accompanied by

a corresponding increase in the ethoxylation number (EON).

The potential use of nonionic surfactants in micellar flooding was also investigated by Verkruyse and Salter (29) using ethoxylated alcohols with n-octane as the hydrocarbon . The phase behavior studies revealed that optimal conditions were obtained at 39.4°C in the absence of salt. Higher salinity systems gave optimal conditions at much lower temperatures; this confirms the earlier findings that present nonionics cannot stand high temperatures. Salter and Verkruyse further performed tests with 1% brine which gave optimal conditions (high solubilization and low IFT) at 37.4°C. Core flooding at this salinity, however, only yielded 56.5% recovery which was well below the anticipated level. Analysis of the effluent indicated that the slug fell apart, resulting in a considerable increase in interfacial tension. A significant surfactant loss was also observed due to partitioning into the oleic phase.

(ii) The second group of publications relating to phase behavior in micellar flooding consists of models. These are mathematical relations developed to relate certain design variables to phase behavior phenomena such as interfacial tension, partition coefficients and solubilization parameters. As with all models describing certain processes their application is limited to the set of conditions or the nature of design variables used, and may not be generalized for other

conditions.

The simplest ones are those of purely empirical correlations of optimal salinity for a given surfactant with several variables such as alkane carbon number, and alcohol type and concentration. Falling into this category is the work by Salager (30). In his work it was shown that the optimum phase behavior for a system containing a nonionic surfactant is obtained when

$$\ln S = k \cdot ACN - f(A) - k.N_{min} \qquad (2.1)$$

where S is % sodium chloride concentration, ACN is the alkane carbon number of the oil-phase at optimum, f(A) is a parameter which gives the effect of alcohol on phase behavior, k is a function of surfactant used and N_{min} is a function of the surfactant chianlength. Another correlation in this category is Huh's relationship at optimal salinity (42):

$$\frac{\gamma^* \sigma^{*2}}{\cos\frac{\pi}{4}} = \text{Constant} \qquad (2.2)$$

It predicts an inverse relationship between the solubilization parameter σ^* and IFT γ^* at optimumal salinty.

The second approach to modelling involves the use of a thermodynamic equation-of-state or the critical scaling theory. This approach is semi-empirical as it prescribes no details about the structure of the microemulsion. In addition, any change in the

component of the system or salinity may cause unpredictable changes. Hence these models only describe the phase behavior of a given system. Prominent in this group is the work of Fleming and Vinatieri (26).

The above model relies on the scaling theory which relates the dependence of physical quantities in the neighborhood of a critical point to the distance from the point, in terms of a set of critical exponents. The interfacial tension at a critical point is related with the following equation :

$$\gamma = \gamma_o |C-C^o|^{\frac{2\nu}{1-\alpha}} \qquad (2.3)$$

where γ is the interfacial tension, γ_o is a scaling factor, C is overall composition, C^o is an adjustable parameter when comparing with experimental results, ν and α are critical exponents, tabulated for different quantities.

The third approach uses statistical thermodynamics which, in principle takes into account molecular interactions between each component and considers explicitly the structure of the microemulsion. Mitchel and Ninham (25) showed that a key factor in understanding microemulsion phase behavior is the geometry of the interfacial surfactant layer. It was shown that the effect of salinity, alcohol and oil can be qualitatively explained by considering this factor only. Extension of Mitchel and Ninham's work was made by Chou and Bae (23). Considering the penetration of alcohol and oil into the interfacial

layer, they developed a model for the solubilization capacity of microemulsions, and optimal salinity.

Given the shortcomings and narrow range of applicability of models, experimental methods were selected for this study. The objective of the study is to investigate the phase behavior of microemulsions using a Saudi Arabian crude oil and a pure alkane with the aim of formulating a microemulsion slug that will produce a high recovery efficiency. Target conditions are 20% salinity and 90°C. The main emphasis will be placed on ethoxylated sulfonates as previous studies showed less surfactant losses with low interfacial tension. The interfacial tension behavior of a crude oil and a pure alkane in the presence of ethoxylated surfactants will be studied under relevant reservoir conditions. As noted by the Texas group (33) and Akstinat (48), these surfactants hold a good promise for EOR.

CHAPTER 3

CHAPTER 3

EXPERIMENTAL

3.1 Materials

The surfactants used comprise of a petroleum sulfonate and two ethoxylated sulfonates which are all anionic surfactants. A nonionic surfactant was also studied. The petroleum sulfonate is TRS10-410, manufactured by Witco Chemical Company. It is a brown and extremely viscous liquid with a rather broad distribution of molecular weight. The equivalent molecular weight ranges from 415 to 430 depending on the batch. Other pertinent properties are given in Appendix A1. This surfactant contains naphtalene and phenanthrene aryl groups, and more than one alkyl chain.

Ethoxylated sulfonates used in this study, V2880 and B1083, are manufactured by Hoechst of West Germany and were received as test samples. These surfactants have ethoxylation numbers 8 and 15, respectively, and are specified to tolerate up to 20% salt with good IFT reduction capabilities. The nonionic surfactant, also manufactured by Hoechst, is SAPOGENAT T-150. Detailed properties of these surfactants are listed in Appendix A1.

Two types of oils were utilized; n-dodecane and a crude oil. The alkane is a product of Fluka AG, Switzerland and is +95% pure. It is a clear liquid at ambient temperature with specific gravity of 0.948 and a

viscosity of 1.414 cp. Its flash point is 74°C. The crude oil was supplied by ARAMCO. Its appearance is dark brown with a viscosity of 6.3 cp at 22°C and 2.3 cp at 90°C. It has a specific gravity of 0.838.

As cosurfactants, straight chain alcohols were utilized. In particular, n-butanol served as the cosurfactant in most of this study. Other alcohols used were n-propanol, n-pentanol and n-hexanol. The physical properties of these alcohols are listed in Appendix A2. Certified ACS grade sodium chloride used to simulate reservoir brine was purchased from Fisher Chemical Company. Distilled water with conductivity 1.5×10^{-6} mhos and surface tension of 71.7 dynes/cm (at 27°C) was used for preparing all solutions.

3.2 Sample Preparation and Equilibriation

In the salinity scan experiments, surfactant solutions containing a fixed percentage of the surfactant and cosurfactant (2:1 ratio by weight) was introduced into 15 ml graduated tubes. A variable concentration of NaCl solution was also added. The resulting solution was mixed to observe the formation or absence of a precipitate. After noting the observation, the oil being studied was introduced into the tubes which were then sealed with teflon tape and capped. The water to oil ratio in this study was always kept at 1:1 ratio and for a total

volume of 15 ml, half of it was occupied by the oil. The solutions were shaken thoroughly and allowed to stand at the desired temperature in an oven of ±1°C precision. Equilibration time was usually 7 days with a little more time allowed for persistent solutions whose phases did not seperate easily.

When surfactant concentrations beyond those allowable by the stock solution were being studied, a slightly different approach was adopted in preparation. In this case, the surfactant concentration was varied by using the concentrated "as received" stock solution of surfactant and pure alcohol in accordance with the surfactant/cosurfactant ratio of 2:1. The rest of the mixing procedure was identical to the one described above. In the study of other variables such as alcohol concentrations and chainlength, all other constituents were kept constant, while varying the one under investigation.

3.3 Interfacial Tension Measurements

The interfacial tensions between the different phases were measured by the spinning drop technique, using the design of the University of Texas (UTSDI model 500). This apparatus makes use of the balance between centrifugal force and interfacial tension. When a drop of a less dense fluid is placed in a denser fluid and rotated in a horizontal capillary tube, the drop becomes elongated along the axis of rotation. Equilibrium is attained when the rotational force is equalled by the interfacial tension between the two fluids.

3.3.1 Use of the Tensiometer

The horizontality of the tensiometer was checked by using an eyeball and leveling screws. The fluids whose IFT was to be measured were introduced into a capillary tube by first filling the tube with the denser fluid, leaving a little void length of about 2 mm. The less denser fluid was then loaded carefully into the tube, ensuring that no air bubbles were present. The amount of the drop placed into the tube was usually 2 microliters. After successfully placing the drop of the less dense fluid, usually oil, the void space in the capillary tube was filled with the denser fluid. The capillary tube was then closed with a teflon cap having a rubber septum.

The O-rings in the teflon cap ensured that the capillary tube was

firmly held in place. To further aid the firm attachment of the tube to the cap, a pendant drop of the denser fluid was left at the tip of the tube. Before inserting the tube-cap assembly in the tensiometer, tissue paper was used to wipe any excess fluid between cap and the tube, in order to avoid flow of any fluid into the rotating parts of the tensiometer that may damage the bearings. Having wiped out any excess fluids a syringe was inserted into the rubber septum through the cap to release any excess pressure caused by the firm attachment of the capillary tube.

The tube-cap assembly was then inserted into the tensiometer slot and screwed firmly in place. The power was turned on to get the motor rotating with tube. Different rotational speeds are possible but extremely low or high speeds were avoided. At the extreme high speed of 9230 rpm droplets became difficult to detach from the end of the tube. This is undesirable because attached droplets are futile for measurements. On the other hand the extreme low rotational speed of 2400 rpm was also avoided since gravity effects cause the deformation of the drop. Thus a rotational speed of around 7000 rpm was utilized.

The target temperature in this investigation, 90°C, was set by pushing down a knob on the tensiometer and screwing it clockwise. Upon releasing the knob, the display showed the current temperature of the tube. Upon heating the tube up to 90°C, as shown on the display, the strobe light was switched on to enable the viewing of the oil

droplet. Rotation of the drop was continued till equilibrium was observed, i.e., till the droplet didn't change its size and shape. It was then maneuvered into a stationary position and readings were taken.

The diameter of the elongated oil drop was measured by moving a bifilar hairlines a short distance below the edge of the drop and then moving them uniformly upward, pausing at the lower end and again at the upper drop edge to record the dial readings. To be able to utilize the infinite drop formula in the calculation of IFT, all drops considered were at least four times longer than their width. Readings of the drop width were continued till two consecutive readings were within ±0.001 cm. Usually not more than ten minutes were required for drop stability as the solutions being measured had already equilibrated for over a week.

As the microscope through which the drops were observed magnifies objects by 2.5 times, the readings of the width were first calibrated. For width readings a drum having 100 divisions was rotated to move the hairline bifilars from one edge to the other. To calibrate this instrument, a one millimeter object was placed inside the tensiometer and the length of the microscope was adjusted such that 10 revolutions of the drum were needed to move the bifilars over the object length; 1000 divisions represent 1 millimeter. The readings on the drum were therefore divided by a factor of 10,000 to convert them to centimeters.

3.3.2 Density Measurements

To calculate the IFT between any two fluids the difference in their densities is required. Densities for all fluids investigated were measured by the weight method. The samples to be measured were first placed in a hot bath, with its temperature adjusted to 90°C. The samples were kept at 90°C for 30 minutes before they were taken by a 500 microliter microsyringe and transferred immediately to a previously weighed vial. The vial was capped and weighed by a Sartorius electronic balance which is accurate to 4 decimal places. The density was obtained in g/cm^3 by dividing the sample weight by 0.5 ml.

3.3.3 Refractive Index Measurement

The refractive index of the denser fluid is another variable required in the calculation of IFT. The refractometer utilized was manufactured by AO Scientific Instruments, Mark II. Before undertaking any measurements, acetone was used to clean the glass surface where samples were placed. After the acetone had evaporated, a drop of the sample was placed on the refractometer and the glass prism placed tightly over it. While looking through the microscopic eyepiece, the straight edge dividing a dark region from a lighted one was adjusted till it was at the intersection of two crossing hairlines. An electronic display showed the refractive index of the fluid under investigation.

3.3.4 Calculation of Interfacial Tension

There are two methods for the calculation of IFT using the spinning drop technique (31),

(1) The finite length method.

(2) The infinite length method.

The expressions used to calculate IFT differ for the two methods by the nature of the elongated drop formed while spinning. If the length of the drop is not at least 4.0 times greater than its width, then the finite length method is used. IFT is then given by:

$$\gamma = \frac{\Delta\rho\omega^2}{4C_d} \qquad (3.1)$$

where $\Delta\rho$ is the density difference between the oil droplet and the aqueous solution, ω is the angular velocity and C_d is determined from tables based on the ratio of the length to width of the rotating oil drop.

On the other hand, when the ratio of length to width of the oil drop is greater than 4.0, which was the case in this study, the infinite drop formula is adopted. By this method IFT is calculated as:

$$\gamma = \frac{\Delta\rho\omega^2 d^3}{32} \qquad (3.2)$$

where d is the diameter of the oil drop in cm $\Delta\rho$, the density difference in g/cc and

ω is the angular velocity in radians/sec. However, if ω is taken in cycles/sec and the measured diameter of the drop is corrected for magnification by refractivity then we obtain :

$$\gamma = \frac{\Delta\rho(2\pi\omega)^2 d^2}{32(RI)^3} \qquad (3.3)$$

where RI is the refractive index of the denser fluid. If ω is taken directly as a period p, displayed on the tensiometer in milliseconds/revolution, then $\omega = \frac{10^3}{p}$. Substituting into the above formula we obtain :

$$\gamma = \frac{\pi^2 x 10^6 x \Delta\rho d^3}{8RI^3 p^3} \qquad (3.4)$$

3.4 Surfactant Concentration by Two Phase Titration

Determination of the surfactant concentration involves the formation of a colored complex between the anionic surfactant and a cationic indicator. The indicator used was a mixture of dimidium bromide and disulphine blue. The titrant HTAB (hexadeycltrimethylammoniumbromide) , a cationic surfactant, complexes with the anionic surfactant. Since the resulting complex is highly insoluble in water, it is dissolved in a nonpolar solvent such as chloroform, hence creating the two phases characteristic of this type of titration.

Initially one milliliter of the solution to be analyzed was taken into a 100 ml stoppered graduated cylinder. It was diluted with distilled water to 20 ml and about 20 ml of indicator solution followed by 15 ml of chloroform and the bottle was shaken thoroughly. At the end of the shaking process, two clear phases developed; an upper greenish oily phase and a pink lower layer. The titrant, $6x10^{-4}$ M HTAB, was added gradually till the pink color in the lower phase just turned clear. The amount of titrant consumed was converted to the actual surfactant concentration through a calibration curve (see Appendix A3).

In the presence of crude oil this technique poses problems mainly due to color interference caused by the oil. Thus, unlike a colorless or bluish endpoint obtained in normal cases, the presence of crude oil produced a certain type of green color. Identification of the exact color required a number of blank tests to be run with different known amounts of surfactants. When large volumes of oil were employed, endpoint identification became impossible. Therefore volumes of solutions less than 0.05 ml were used for analysis. The mass balance obtained on different phases proved the accuracy of this technique.

3.5 Viscosity Measurements

The viscosity of the middle phase microemulsion was measured using the Contraves Low Shear viscometer. The equipment is attached to a

constant temperature digital Haake bath to enable viscosity determination at high temperatures. After achieving the set temperature the viscometer was turned on and the 'range' and 'step' adjusted. For most of the study the range was kept at 5 and the step at 25 (shear rate of 25.5 sec^{-1}).

The viscometer operates on the principle of shearing between two concentric circles. As such, the sample to be measured was introduced into a metallic bowl with a cylindrical hollow. A pin was then selected with a corresponding cylindrical bulb that fits into the bowl. It was attached to a lever arm that allowed its immersion and removal from the bowl. After immersing the pin into the bowl and making sure it was concentric with the bowl, the viscometer motor was started, to rotate the bowl. The shearing force generated was shown by a digital display. Multiplication of the displayed number by a conversion factor (see Appendix A) corresponding to the set range and step, yielded the viscosity of the sample in centipoise.

3.6 Determination of Critical Micelle Concentration (CMC)

Surface tension technique was utilized for measuring the CMC of the ethoxylated sulfonates studied in the absence of electrolyte . Samples with known surfactant concentration were used in surface tension measurements. The Kruss made K10 digital tensiometer was used with

the ring method. To ensure cleanliness, the ring was cleaned each time with acetone and then with alcoholic potash followed by distilled water. Finally the ring was flamed in a bunsen burner. The measured surface tension values were plotted against surfactant concentration. Critical micelle concentration was taken to be the intersection of the two straight lines connecting the surface tension values.

3.7 Phase Boundary Delineation by Ultraviolet Light

The opaque nature of crude oil precludes identification of the boundary between the oleic and microemulsion phases. However, the use of ultraviolet light helps overcome this problem. Under the ultraviolet light , crude oil is recognized by its green color while microemulsion appears bluish-green. The aqueous phase displays no color and can easily be distinguished from the other phases.

3.8 Cloud Point Measurements

The upper limit for surfactant solubility is termed the cloud point (38). At this point the bonds holding the ethoxy chain is nullified and the surfactant aquires a water insoluble form. The cloud point is a function of both surfactant and electrolyte concentrations. Cloud point experiments were carried out for ethoxylated sulfonates (V2880 and B1083) and a nonionic surfactant (T150) with zero or certain concentration of n-butanol. 10 ml of known concentration of surfactant

having zero or certain concentration of NaCl and n-butanol were introduced into 20 ml vials. These vials were kept in a thermostated water bath without shaking. The bath temperature was increased gradually and the cloud points (phase separation temperature) of the surfactants were determined as a function of temperature by observing the onset of precipitation/turbidity development visually.

CHAPTER 4

CHAPTER 4

RESULTS AND DISCUSSION

Several unique features of phase behavior have been observed under the target conditions of high temperature and high salinity. The results showed that while petroleum sulfonates produce low optimal salinity both for dodecane and crude oil, the ethoxylated sulfonates exhibited high tolerance to salt even at elevated temperatures. The nonionic surfactant gave unacceptably high IFT's and was not investigated further. The results and accompanying discussion of this study will be presented in the following order:

4.1 Interfacial Tension Behavior of TRS10-410

4.2 Interfacial Tension Behavior of a nonionic surfactant

4.3 Phase Behavior Studies with ethoxylated sulfonates

4.4 Ternary Diagram Representations

4.1 Interfacial Tension Behavior of TRS10-410

Petroleum sulfonates have been extensively used in phase behavior studies. Thus the objective of using a petroleum sulfonate was merely to demonstrate the methodology to be used and also to reproduce the available literature results with pure alkanes. Along this line

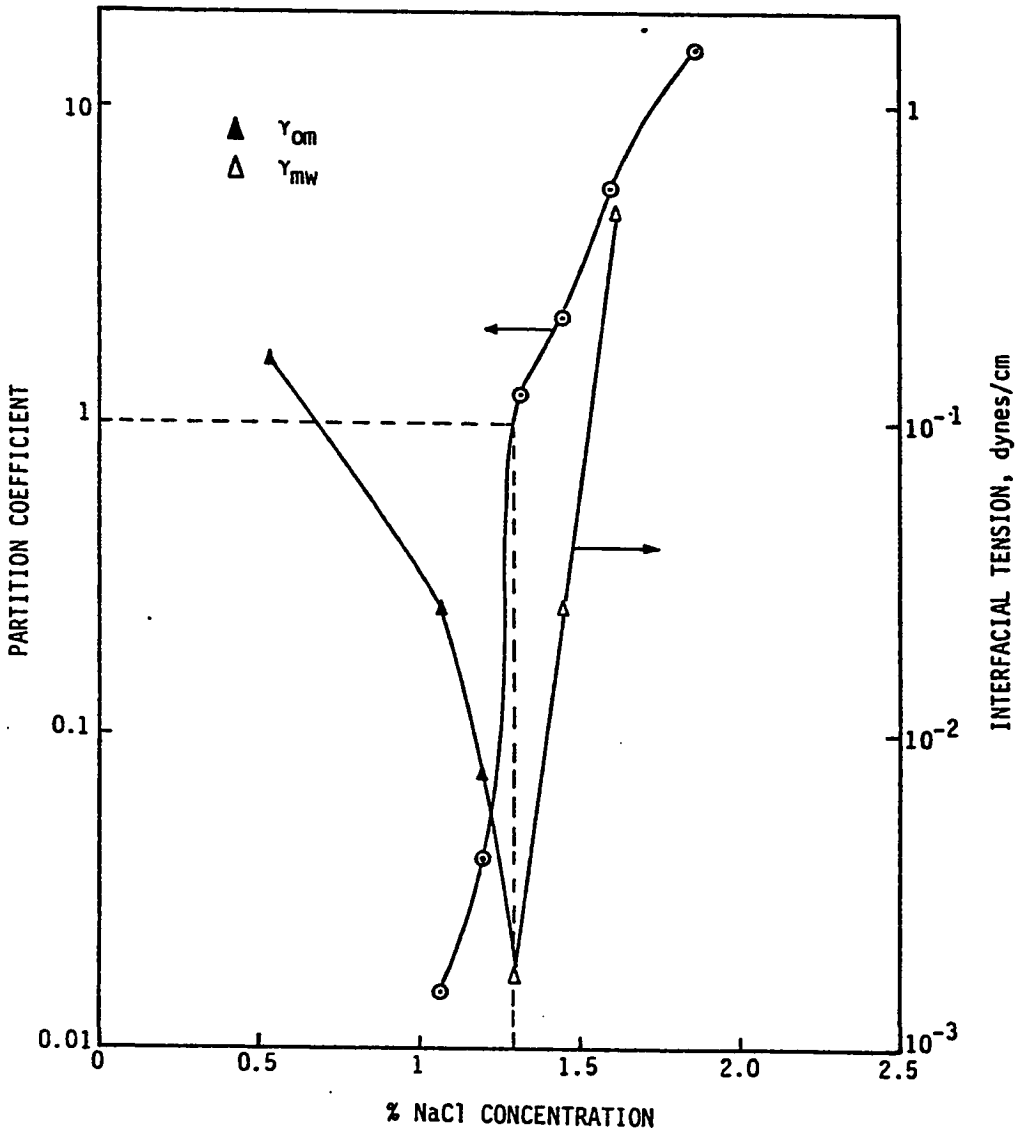

Fig. 1: Effect of Salinity on IFT and Surfactant Partition Coefficient for 4% TRS-410 + 2% n-Butanol + NaCl + n-Dodecane System.

TRS10-410, a petroleum sulfonate, was investigated for its IFT lowering capability using dodecane and crude oil. Results of IFT against salinity are presented in Fig. 1 and also in Table 1 in Appendix B, where dodecane was used as the oleic medium at room temperature. The IFT between oil and microemulsion, γ_{om}, decreases as salinity increases, while that between the microemulsion and brine, γ_{mw}, increases. The two plots intersect at a salinity defined as the optimal salinity which occurs at 1.3 wt %. This value is in agreement with the published values (6). Figure 1 also illustrates the partition coefficients defined as the ratio of surfactant concentration in oil to that in brine C_o/C_w. The partition coefficient is a measure of the level of interfacial activity and unit partition coefficient is observed to correspond to a salinity of 1.3 wt % which also coincides with the optimal salinity obtained by IFT measurements. Hsieh (6) studied a similar system of 5% TRS10-410 with 3% n-butanol. An optimal salinity of 1.5 wt % brine was obtained; this is comparable to 1.3 wt % for 4% TRS10-410 and 2% n-butanol used in this study.

The interfacial tension behavior of this surfactant was further investigated with crude oil at room temperature. Results of IFT against salinity are shown in Fig. 2 and Table 2 in Appendix B. Interestingly, the crude oil exhibited a similar behavior as the dodecane described above. In Fig. 2 the interfacial tension between the excess-oil and excess-brine phases is plotted versus salinity. In contrast to the

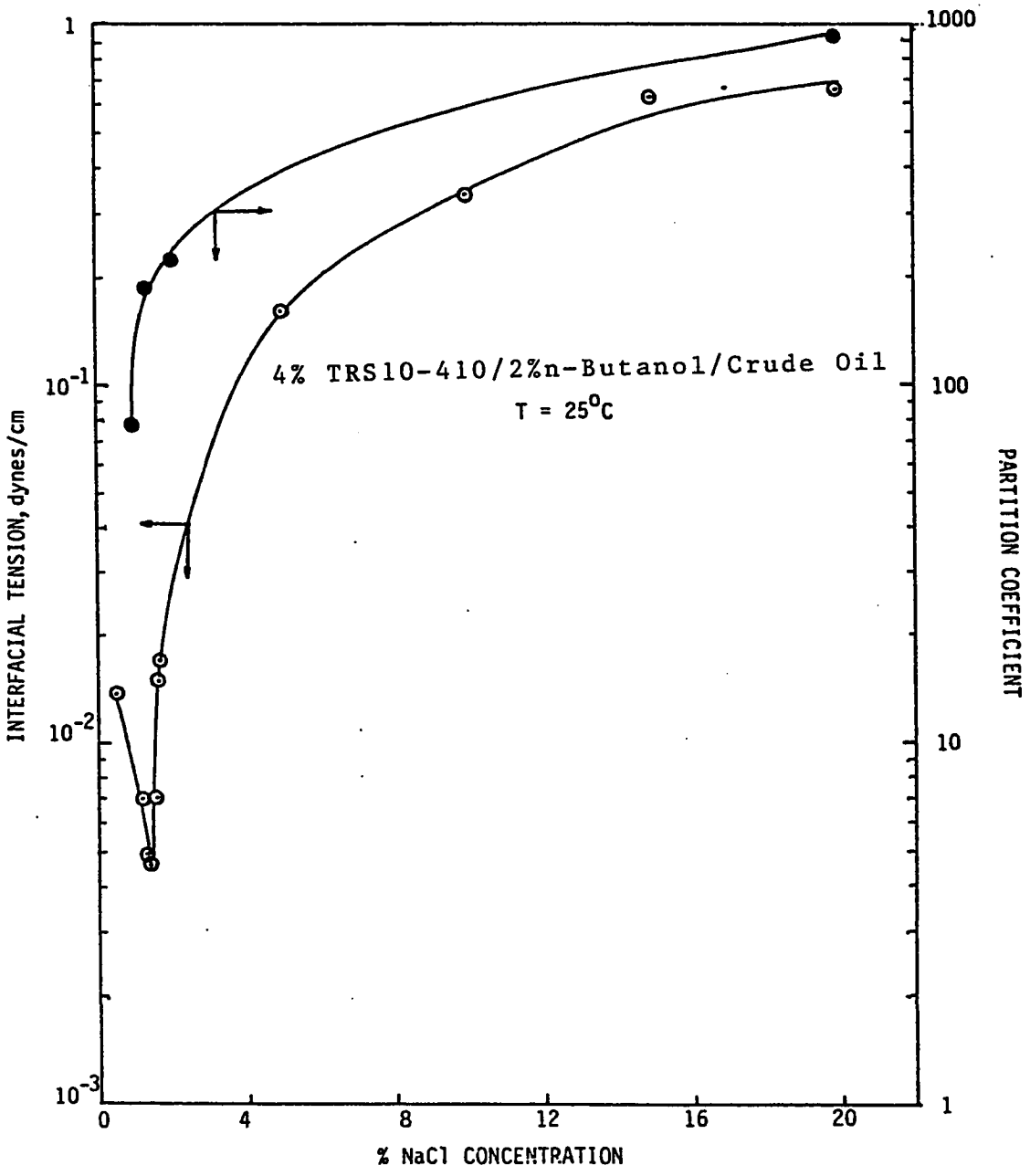

Fig. 2: Effect of Salinity on IFT and Surfactant Partition Coefficient for TRS 10-410/Crude Oil System.

dodecane study, the middle phase microemulsion was not used in IFT determination as the strobe light on the tensiometer could not easily penetrate it. A minimum in IFT for this system is observed at 1.4 wt % NaCl, close to that obtained in the dodecane system. The minimum in IFT occurs at 4.6×10^{-3} dyne/cm and beyond this value IFT increases for all salinities scanned up to 20% NaCl. On the other hand, the partition coefficients shown in Fig. 2 exhibit rather high values indicating that the aqueous phase is practically devoid of surfactant.

The mechanism of formation of middle phase can be schematically illustrated in Fig. 3. It should be noted the oil droplets in the middle phase coalesce to form oil external microemulsion in cylinders 6 and 7. Increase in the salinity decreases the CMC and concurrently increases the aggregation number of micelles which in turn lead to enhanced solubilization of oil within micelles. Compression of the electrical double layer around the micelles reduces the surface charge of micelles causing the droplets to approach each other through the van der Walls attraction forces. With increasing salinity, the density of micelles decreases due to enhanced solubilization of oil in them whereas the density of brine increases. It is these forces that drive the oil droplets into the water-external microemulsion phase (38).

Figure 4 illustrates the phase types corresponding to the tubes in Fig. 3. The lower tubes with two phase represent type I whereas the upper ones with two phase describe type II. In the region of middle

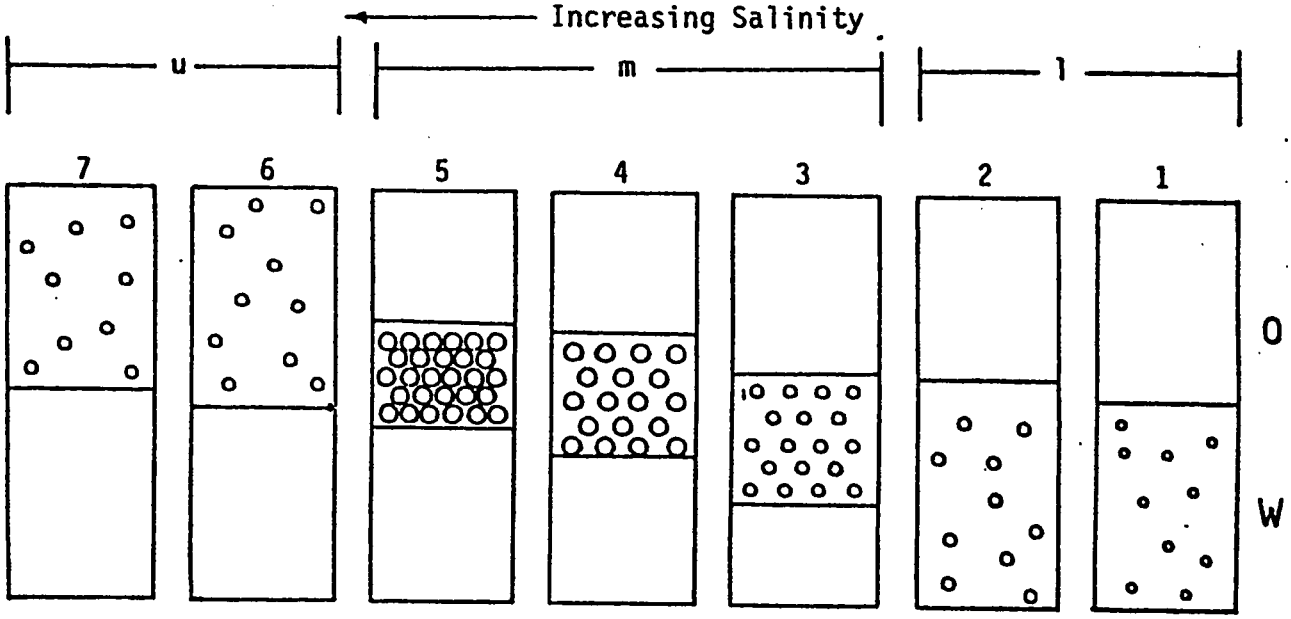

Fig. 3 : A Schematic Illustration of the Effect of Salinity on the Phase Behavior of TRS-410/n-Butanol/Dodecane/ NaCl System (Ref. 8).

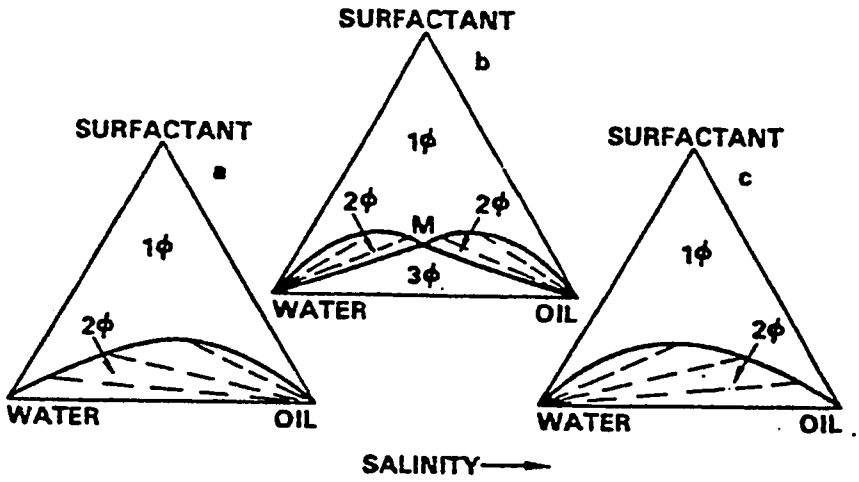

Fig. 4: Illustration of Simple Phase Behavior and Winsor's type I, III and II Systems.

phase formation the phase behavior can be described by (b) or type III. The IFT behavior of TRS10-410 with dodecane and crude oil revealed that the petroleum sulfonate produced very low optimal salinities, i.e. in the vicinity of 1.5%. However, at our target conditions of 20% salinity this surfactant yields unacceptably high IFT's.

Nevertheless, before it was relegated from further high salinity study, a high temperature investigation was conducted using dodecane. The surfactant formulation was composed of the same conditions as before - 4% TRS10-410/2% n-butanol, with a WOR of unity. A plot of IFT against salinity is shown in Fig.5. Similar to the room temperature results, an optimal salinity of 2.5% with relatively high IFT was observed for the high temperature study. The above observations revealed that petroleum sulfonates give low optimal salinities for both low and high temperature studies. Other surfactants were therefore considered for further studies with the aim of lowering IFT at high salinity levels.

4.2 Interfacial Tension Behavior of a Nonionic Surfactant

Before continuing the study of phase behavior with other types of anionic surfactants, a nonionic surfactant, Sapogenat T-150, was tested for its ability to lower IFT at the aqueous/oil interface. It is widely believed that nonionic surfactants adsorb less on reservoir rocks due to the absence of ionic moities in the surfactant molecule. Below their

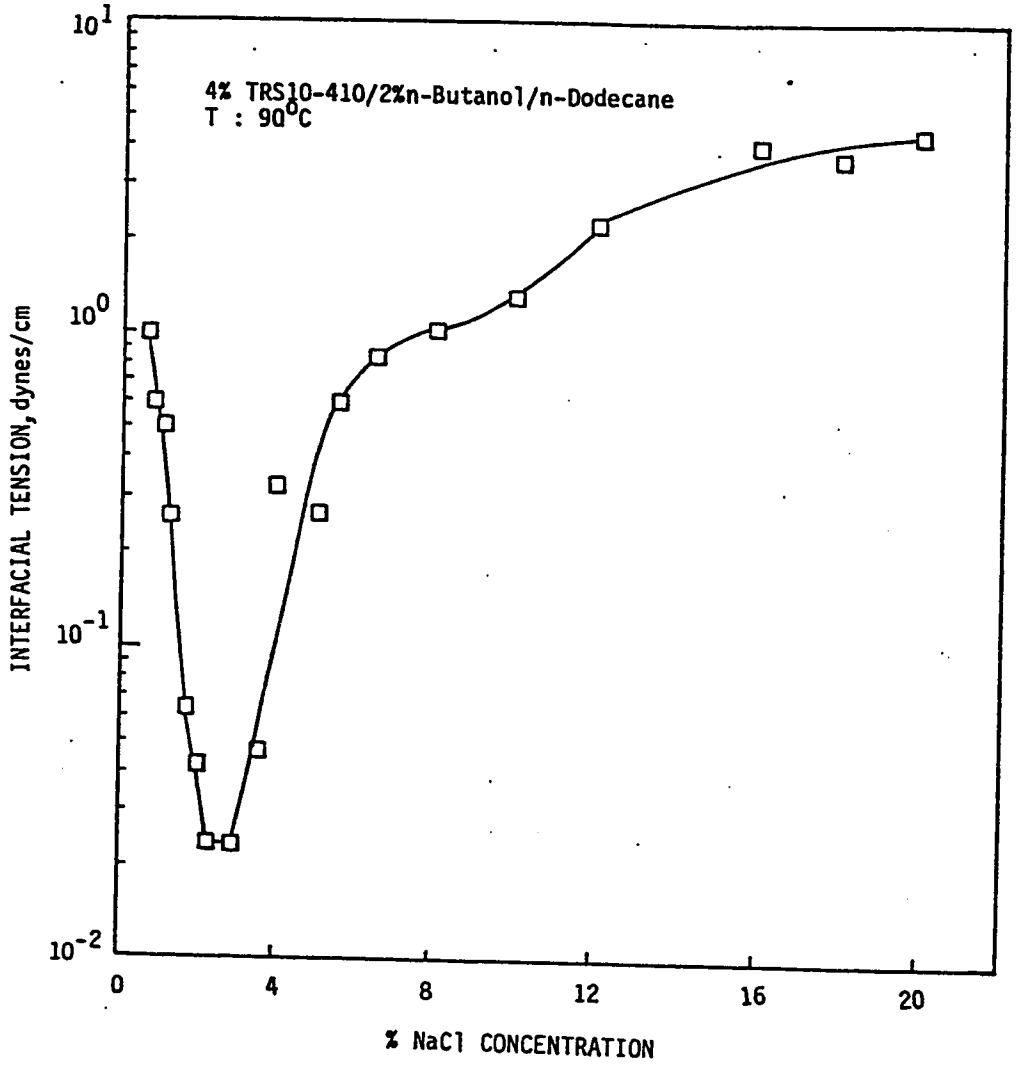

Fig. 5: Effect of Salinity on IFT of TRS10-410/n-Dodecane System.

cloud point, nonionics are also tolerant to harsh reservoir brines, i.e., they do not precipitate at high salinities. With these qualities, a good IFT lowering capability would make them ideal candidates for micellar flooding.

However, as shown in Fig. 6, intolerably high IFT's result from the use of the nonionic surfactant (Sapogenat T-150) with crude oil at 90°C. In this study, the concentration of surfactant was kept constant at 4% by weight while salinity was varied from 1 to 22%. The plot of IFT as a function of salinity shows that IFT increases continuously with increasing salinity.

As noted by Gracia et al (19) most commercial nonionics produce high IFT and low solubilization. Above all, they cannot withstand high temperature. The result of Fig. 6 at a high temperature of 90°C is therefore consistent with earlier findings. However, through proper structural design nonionics can be tailored to withstand higher temperatures.

4.3 Phase Behavior Studies with Ethoxylated Surfactants

Every surfactant class generally produces different optimal salinity. For example, petroleum sulfonates yield lower optimal salinity than many surfactant classes. However, a major objective of low-tension micellar flooding is the design of surfactants for high-salinity and high-

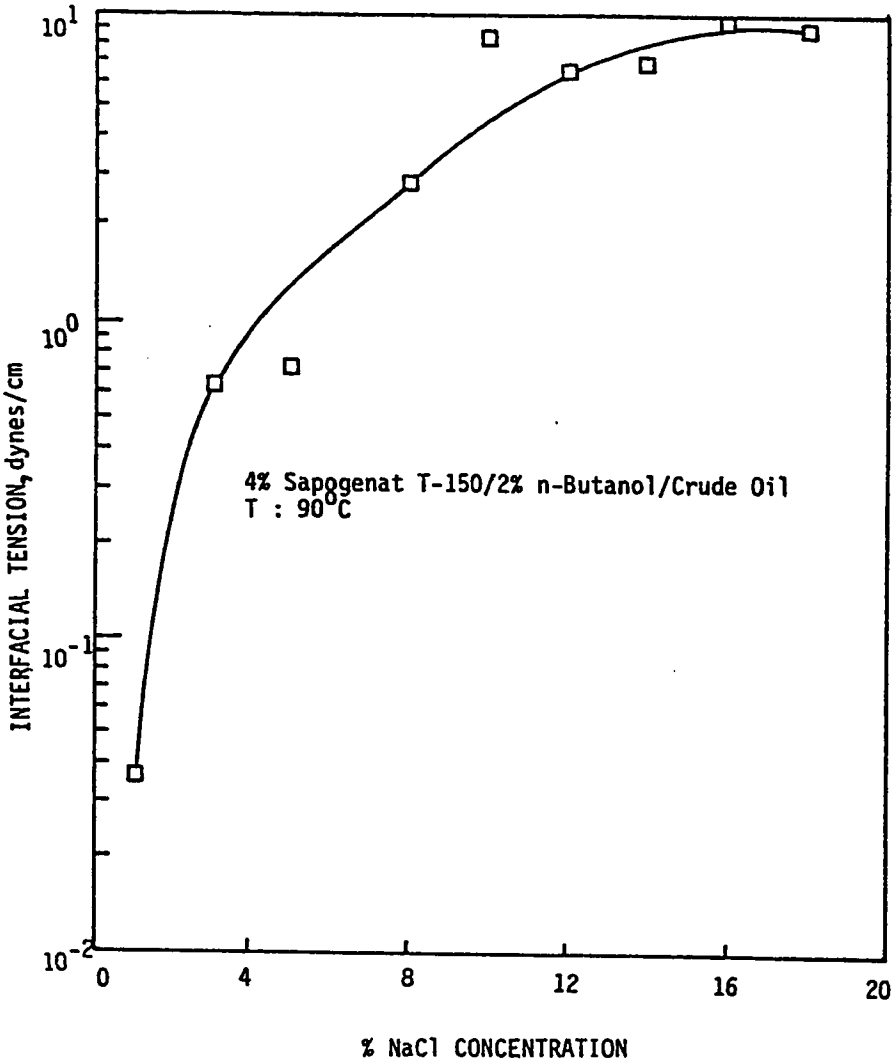

Fig. 6: Effect of Salinity on IFT of Sapogenat T-150/Crude Oil System.

temperature reservoirs. While there has been a considerable success in the salt tolerant surfactants, e.g. ethoxylated sulfonates, surfactants that are stable at both high-salinity and high-temperature are still in the development stage.

Presently, however, ethoxylated sulfonates seem to be good candidates for the micellar flood designers, under harsh reservoir environments. The applicability of various surfactant types in micellar flooding is illustrated in Fig. 7 (49). Evidently, ether sulfonates together with aromatic/aliphatic sulfonates appear to hold great promise at hostile reservoir conditions. For this reason, the remaining of this study was conducted with ethoxylated sulfonates.

Critical Micelle Concentration of Ethoxylated Sulfonates

The critical micelle concentration is the concentration of surfactant at which the surfactant monomers begin to aggregate in the form of micelles. The formation of micelles represents an important interfacial activity because they eventually lead to formation of microemulsion and in turn to reduction in IFT. Most measurable properties in surfactant solutions containing micelles exhibit an unusual behavior indicative of their presence. Specific conductivity, surface tension, osmotic pressure, etc., all show a break at concentrations corresponding to the onset of micelle formation. The micelles are generally considered to be

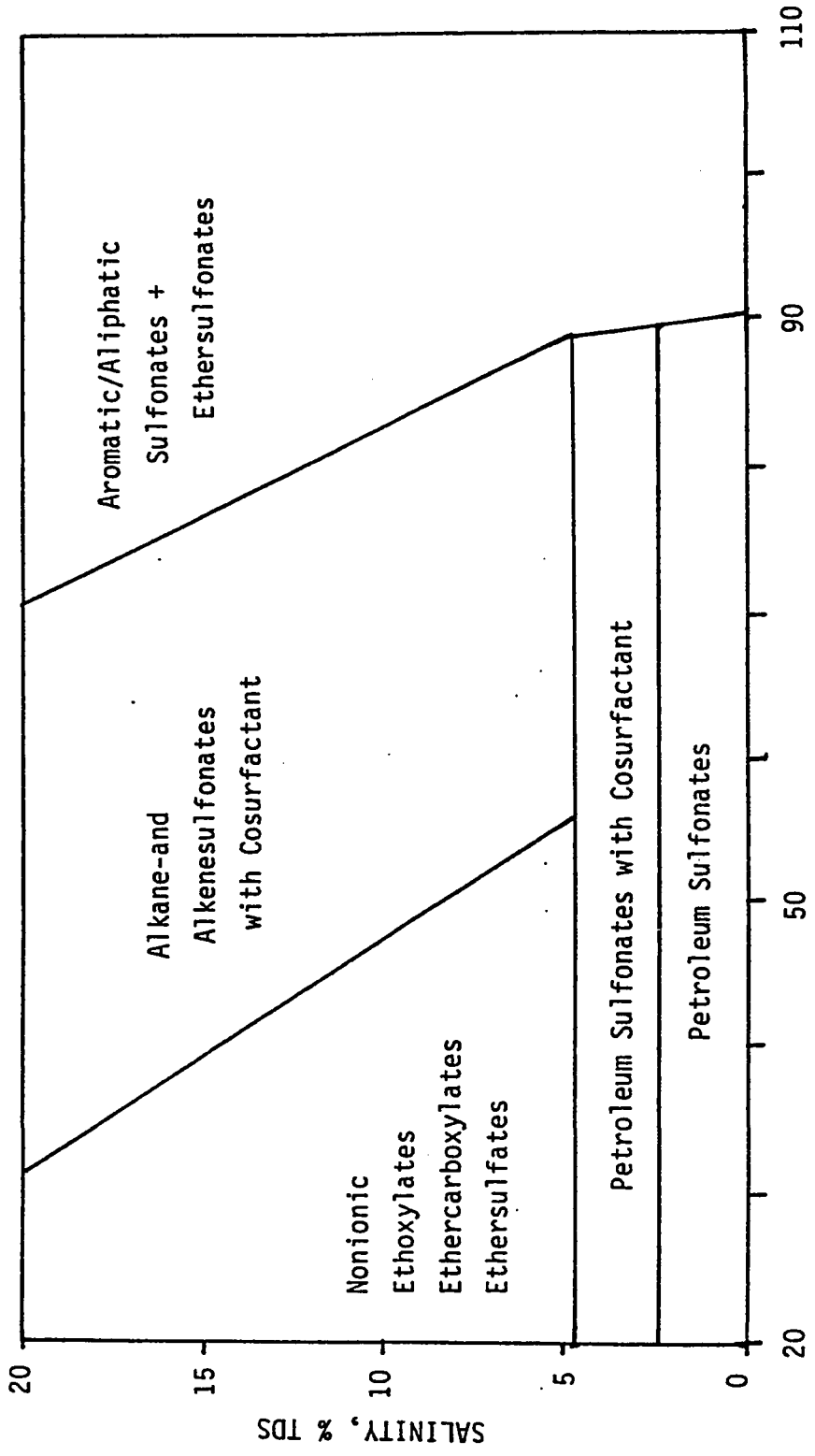

Fig. 7 : Applicability of Surfactant Types in Micellar Flooding (Ref.49).

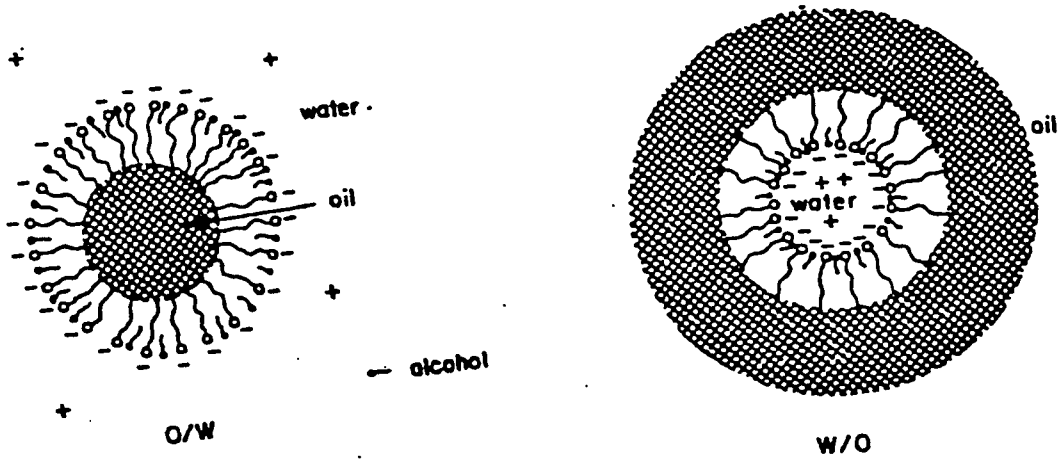

Fig. 8: Illustration of the Oil-in-water and Water-in-Oil Type Microemulsions. (Ref. 38).

spherical about 40-100 Angstrom in diameter.

Every surfactant micelle has a different aggregation number as dictated by the size and geometry of the micelle (34). One of the important properties of micelles is their ability to dissolve certain substances that are normally insoluble in a given medium. Microemulsion droplets can similarly form through incorporation of oil, alcohol and water molecules in a manner shown in Fig. 8.

The critical micelle concentrations for V2880 and B1083 shown in Fig. 9 were determined by the surface tension method. The point at which the surface tension levels off as surfactant concentration is increased was taken as the CMC. The two surfactants, V2880 and B1083, respectively yielded CMC values of 0.021 g/l and 0.043 g/l. It may be noted that the CMC for B1083 is higher than that of V2880. The data on CMC versus ethoxylation number of ethoxylated sulfonates presented in Fig. 10 shows that increasing the EO number increases the CMC; this is in line with the respective surface activity of ethoxylated sulfonates and also in agreement with the literature data (35).

Cloud Points of Ethoxylated Sulfonates

Ether sulfonates consist of a hydrophobic alkyl/aryl group and a hydrophilic ethoxy chain with the sulfonate group attachment. The solubility of hydrophilic (nonionic) part in water is dependent upon

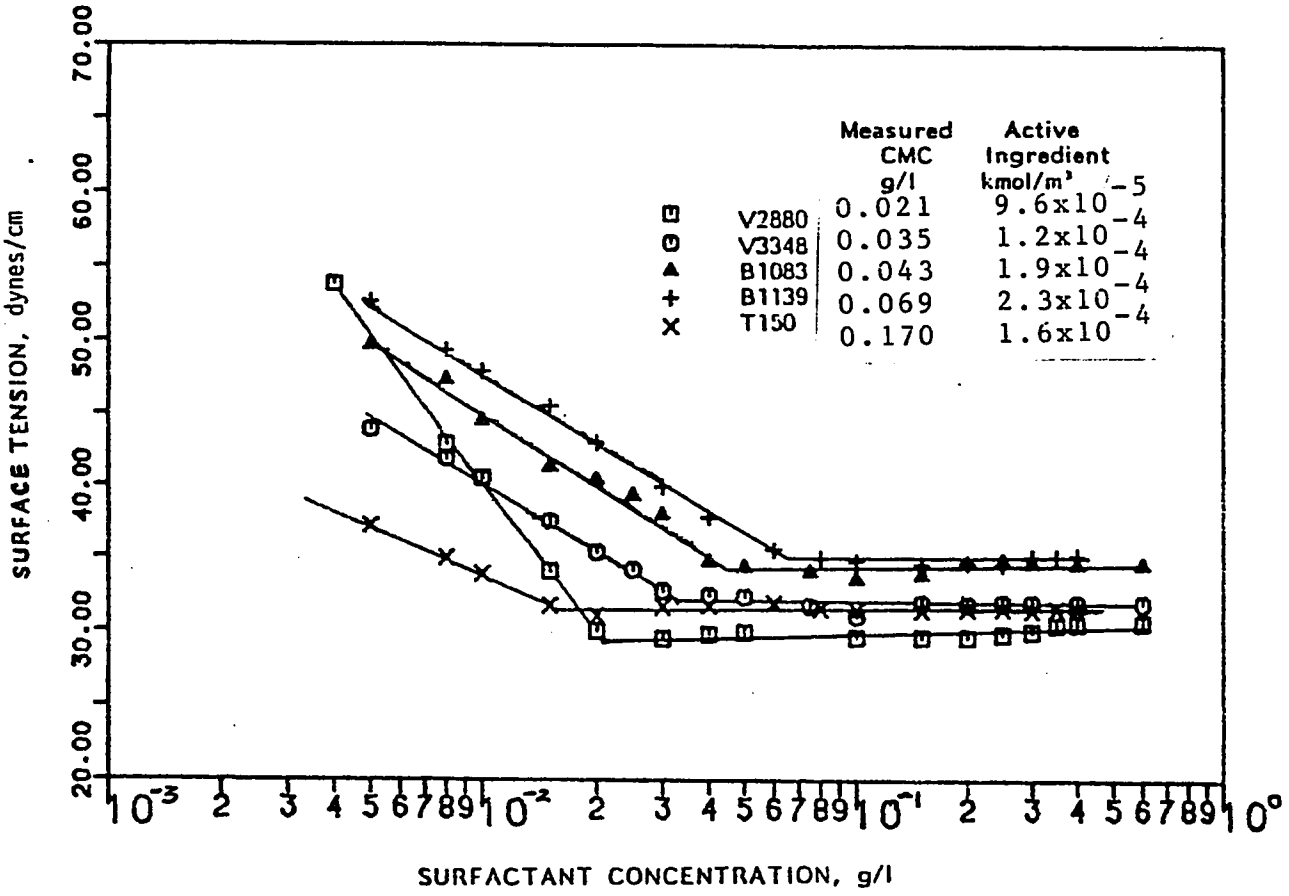

Fig. 9: Plot of Surface Tension vs. (Surfactant Concentration) for Various Ethoxylated Sulfonates at Room Temperature.

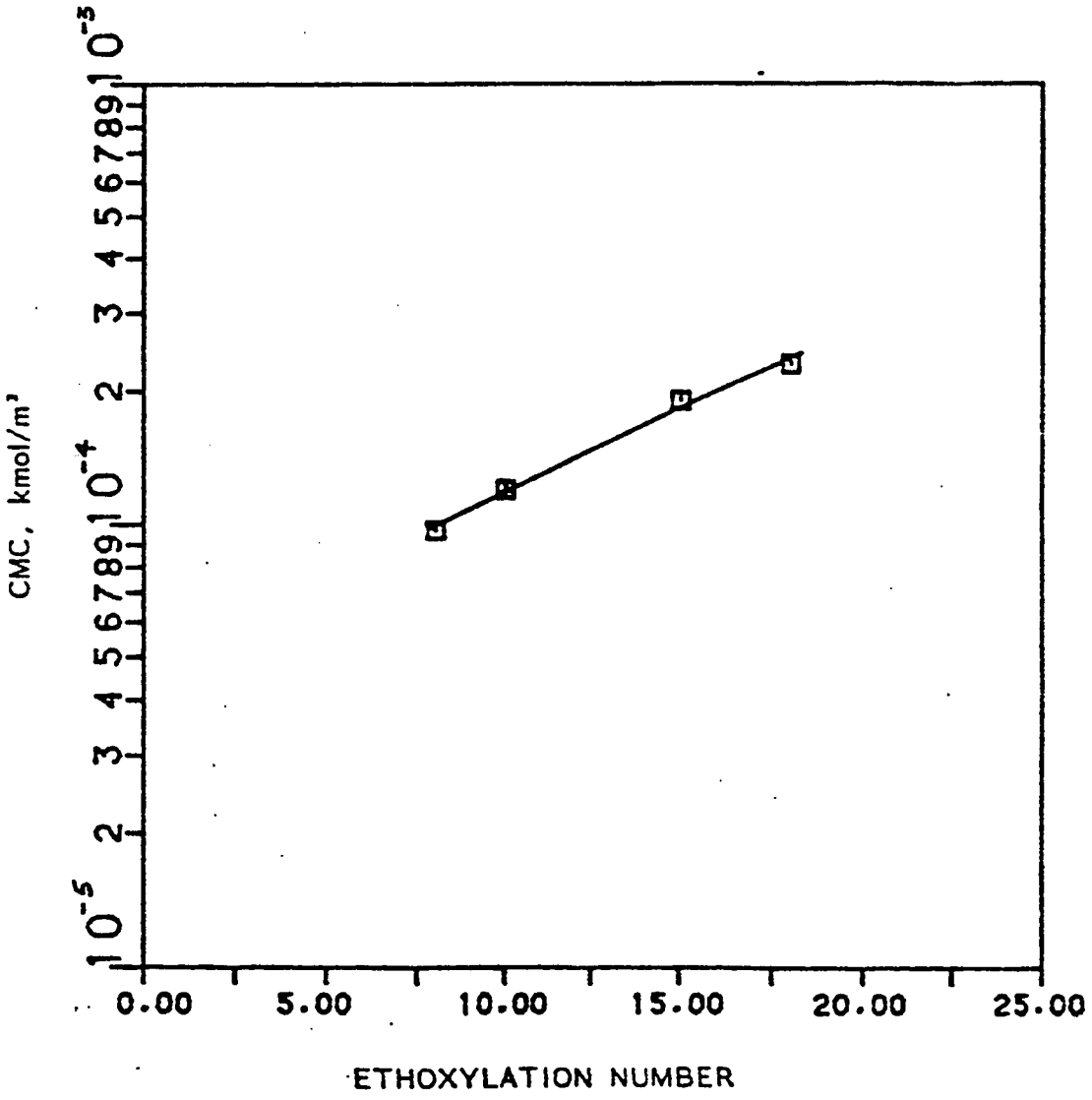

Figure 10: Plot of (CMC) vs. Ethoxylation number for Ethoxylated Sulfonates at Room Temperature.

hydration of the oxygen groups by hydrogen bonds. The longer the EO chain is the greater is the water solubility of the ethoxylate. The bond holding the ethoxy chain, however, is reversible and nullified upon heating. At high temperatures, the water molecules are broken and acquire a water insoluble form. The temperature at which this cloudiness appears is called cloud point (36).

The cloud point is rather sensitive to the concentration of salt. Ethoxylated sulfonates, unlike nonionic surfactants, are better salt tolerant and also more temperature stable compared to ether phosphates, ether sulphates or ether carboxymethylates (36). The position of the ethoxy and sulfonate groups significantly affects the properties of these surfactants. In this study, the cloud point of ethoxylated sulfonates and a nonionic surfactant has been investigated in the presence of NaCl and n-butanol using turbidity method as described previously (38).

Data obtained on the phase separation temperature of various surfactants as a function of salinity and surfactant concentration with and without n-butanol are presented in Table 11a, 11b and Fig. 11. It is apparent that all the surfactants tested so far have PST of less than 90°C at 20% NaCl concentration. It is also clear from Fig. 11 that the dependence of surfactant concentration on the phase separation is almost nil. Similar results have been reported in the literature (39).

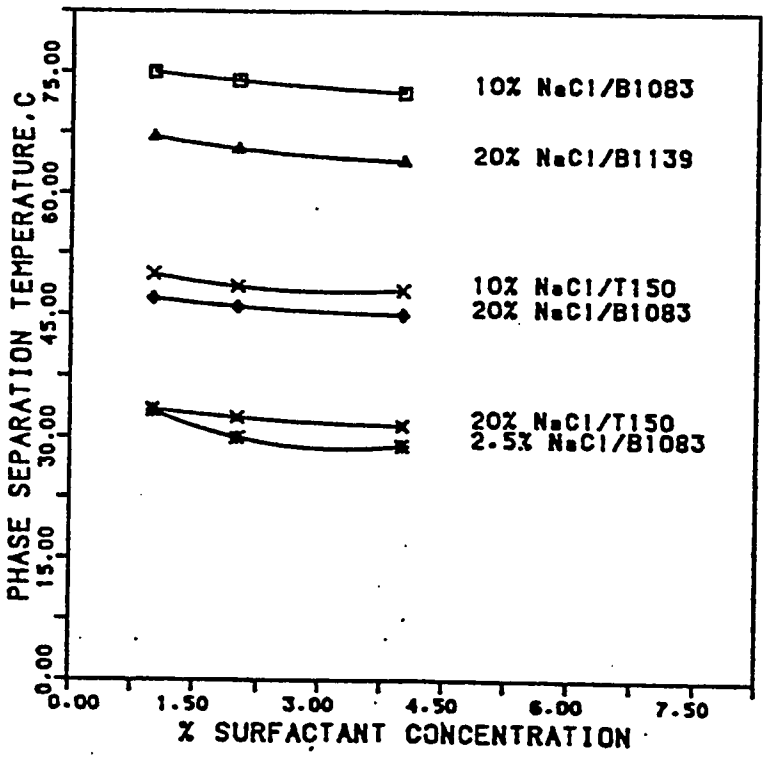

Fig. 11: Phase Seperation Temperatures of Various Surfactants at Different Salinities.

The results discussed above demonstrate that even though ethoxylated sulfonates and nonionics are better tolerant surfactants, commercial companies can tailor more suitable surfactants to improve their solubilities at high temperature. Of course, IFT lowering must also be considered as a prime target.

Phase Inversion Temperature of V2880

As phase behavior is a strong function of temperature, this experiment was conducted to find the temperature at which surfactant micelles would change from one state to another. To achieve this, the interfacial property of equilibrated surfactant-crude oil systems was studied at different temperatures. The phase inversion temperature (PIT) is found to occur at a particular temperature corresponding to a minimum IFT (9). PIT generally increases with increasing equivalent alkane carbon number (EACN) of the oil with decreasing salinity and with increasing EO number of ethoxylated surfactants. Below the PIT, the emulsion is O/W whereas above PIT it is W/O. Figure 12 illustrates the determination of the PIT for V2880 at 20% salinity. The PIT takes place at 35°C corresponding to an IFT value of 8.4×10^{-3} dynes/cm.

The formation of liquid crystals has been shown to depend on temperature (22). For a given surfactant composition the transition

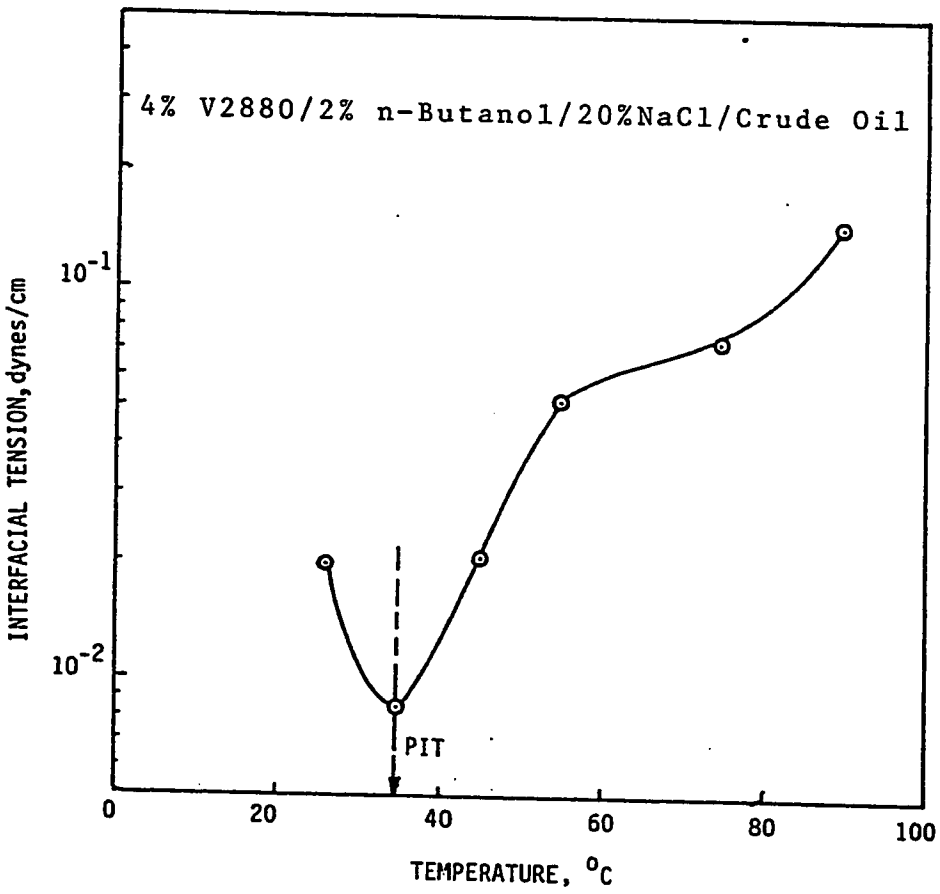

Fig. 12 : Determination of Phase Inversion Temperature for V2880 (WO=1).

between microemulsion and liquid crystals occurs at low temperatures. Since the formation of gelly liquid crystals is detrimental to any flooding process, the phase inversion temperature must be used as a guide, to avoid their formation. In this study, the middle phase appeared as microemulsion at 90°C. However , it became jelly upon removal from the oven to the laboratory temperature of 22°C .

Interfacial Tension Behavior of V2880 with Crude Oil (salinity scan)

In order to evaluate the IFT lowering capacity of this ethoxylated sulfonate, 4% V2880 and 2% n-butanol were equilibrated with crude oil at various salinites. Figure 13 shows a plot of IFT against salinity for this system. Since the microemulsion could not be used for IFT measurement for reasons explained earlier, the IFT was determined between the oleic and aqueous phases as justified below.

If the IFTs obey Antonoff's rule, the tension between the aqueous and oil phases is the sum of the tensions between the other two phases (24).

$$\gamma_{AO} = \gamma_{AM} + \gamma_{OM} \qquad (4.1)$$

where A, M and O respectively represent the aqueous, middle and oil phases. Even if this relationship does not hold exactly, the AO tension is the largest of the three and becomes minimum at the optimal salinity

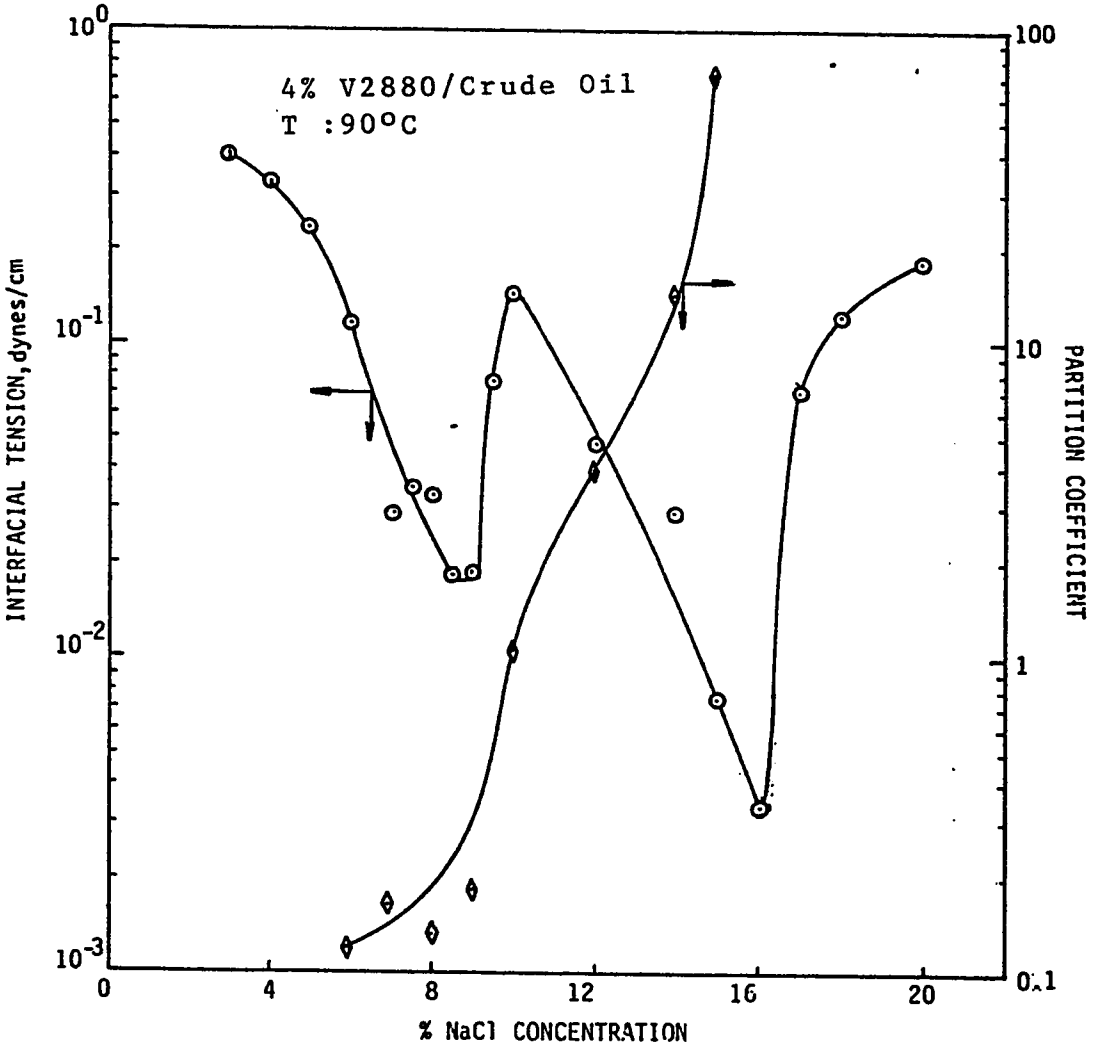

Fig. 13 : Effect of Salinity on IFT and Surfactant Partition Coefficient.

where the other two tensions are equal. Thus the IFT values given in Fig. 13 are the maximum tension values and are at least twice larger than the actual values. Seeto et al (44) have shown that the Antonoff's rule, though complicated, holds true under most conditions, particularly in systems of three-phase formation.

As depicted in Fig. 13, the first minimum occurs at 9% salinity and the second at 16% salinity. A plot of partition coefficients on the same figure shows that unit partition occurs around the first minimum. While the occurrence of a minimum at 9% salinity may be explained by the classical middle phase formation theory, the mechanism leading to the formation of the secondary minimum is a subject requiring further investigation.

Interfacial Tension Behavior of V2880 with Dodecane (salinity scan)

The effect of salinity on the interfacial tension of V2880 is presented in Fig. 14. The interfacial tensions between the oil and the aqueous phases exhibit two minima, one at about 8% NaCl concentration and the other at approximately 14% salinity. While the first minimum corresponds to the classical three-phase region in Winsor's type III diagram, no mention of the second minimum is believed to exist in the recent literature (40-46). The solutions in the secondary optimal salinity region exhibit three phases with a distinct middle phase similar to those

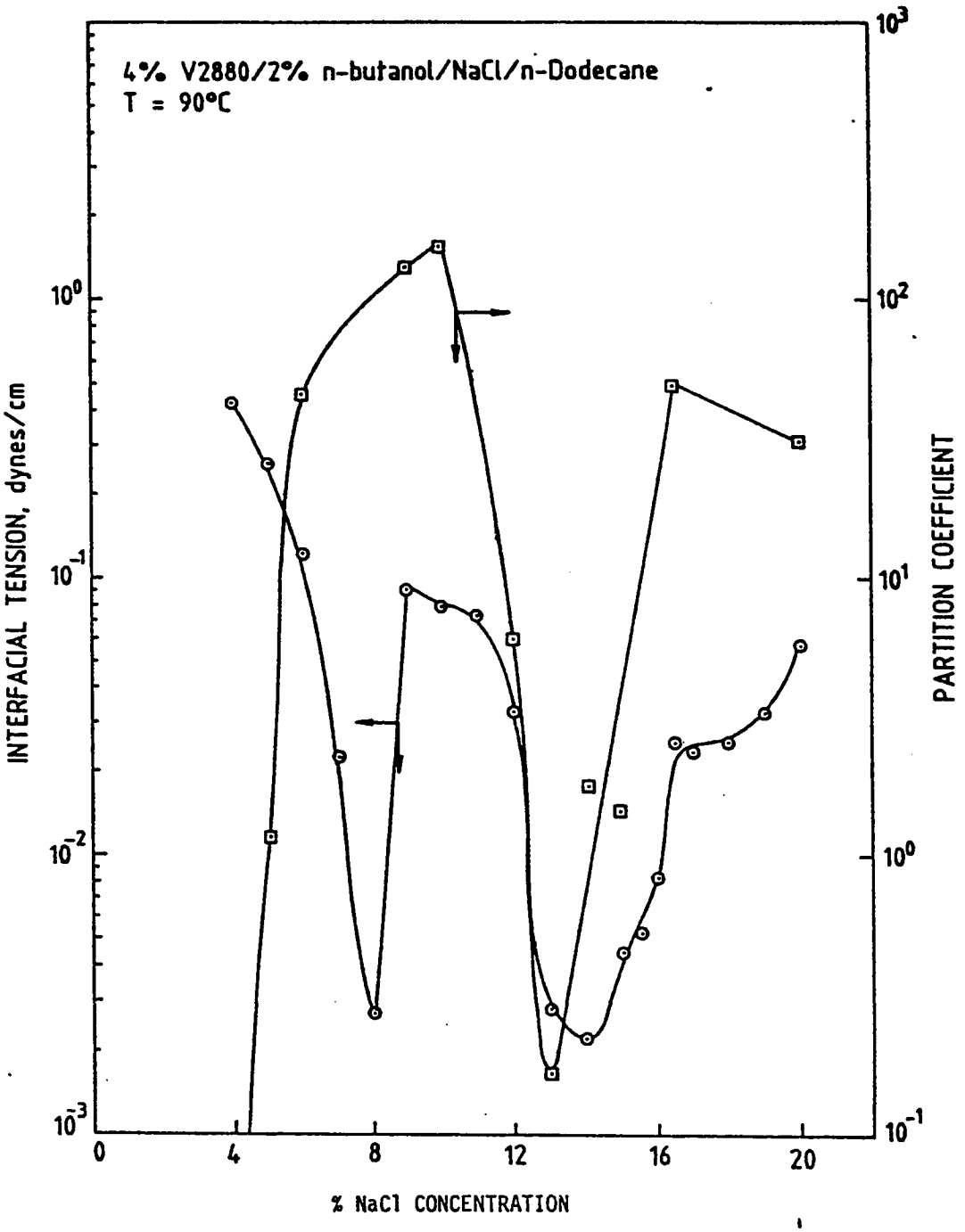

Fig. 14: Effect of Salinity on IFT of V2880/n-Dodecane System.

obtained in the primary optimal salinity region. The presence of the secondary optimal salinity at 90°C is extremely important for high salinity and high temperature oil reservoirs as it can be favorably utilized in the design of appropriate surfactants.

Partition coefficients as measured by C_{oil} / $C_{aqueous}$ given in Fig. 14 also follow an intriguing behavior. A partition coefficient of about unity coincides with the primary optimal salinity. Interestingly the secondary optimal salinity also occurs at close to unity. The presence of the minimum in IFT at the primary optimal salinity is generally in agreement with many published data (3,8,16). However, the minimum observed at the secondary minimum is believed to be reported for the first time.

The mechanism of the minimum in the three-phase region, the primary minimum, has been attributed to the critical phenomena and the existence of critical endpoints (24,16,45). The secondary minimum, on the other hand, can be explained on the basis of a thin interfacial layer between the oil and aqueos phases. Over 90% of the surfactant was found to accumulate in this layer constituting about 2 to 4% of the total volume. The infrared analysis of the middle phases corresponding to 8% and 14% NaCl concentrations indicates striking similarities. Both samples show the presence of surfactant, n-dodecane, n-butanol and water which are the necessary ingredients for microemulsion formation. However, the infrared spectra for the latter sample reveal increasing

concentration of surfactant, n-dodecane and n-butanol in a much smaller volume. Even though the structure of the microemulsion in the primary optimal salinity has been identified as water-external (38) that at the secondary minimum is unknown at present. The infrared data coupled with partition coefficient measurements indicate that with increasing salinity higher levels of surfactant are salted out into the interfacial layer forming most likely an oil-external microemulsion. Moreover, at 14% salinity the phase inversion temperature of the surfactant is much less than 90°C again suggesting the formation of a W/O type microemulsion.

Effect of Alcohol Concentration on IFT in V 2880/Crude Oil System

Since alcohol is an indispensable component in the formulation of most microemulsions, a study was initiated to investigate the effect of alcohol concentration on IFT lowering. It should be noted that all previous results were obtained using a surfactant alcohol ratio of 2/1. The data shown in Fig. 15 indicate that increasing the alcohol concentration increases the IFT. This observation is consistent with Hsieh's work (6), in which he noted that, increasing isobutanol concentration decreases the solubilization capacity of the TRS10-40 containing microemulsion. Since solubilization is a measure of the interfacial activity, this implies a reduction in IFT lowering capacity.

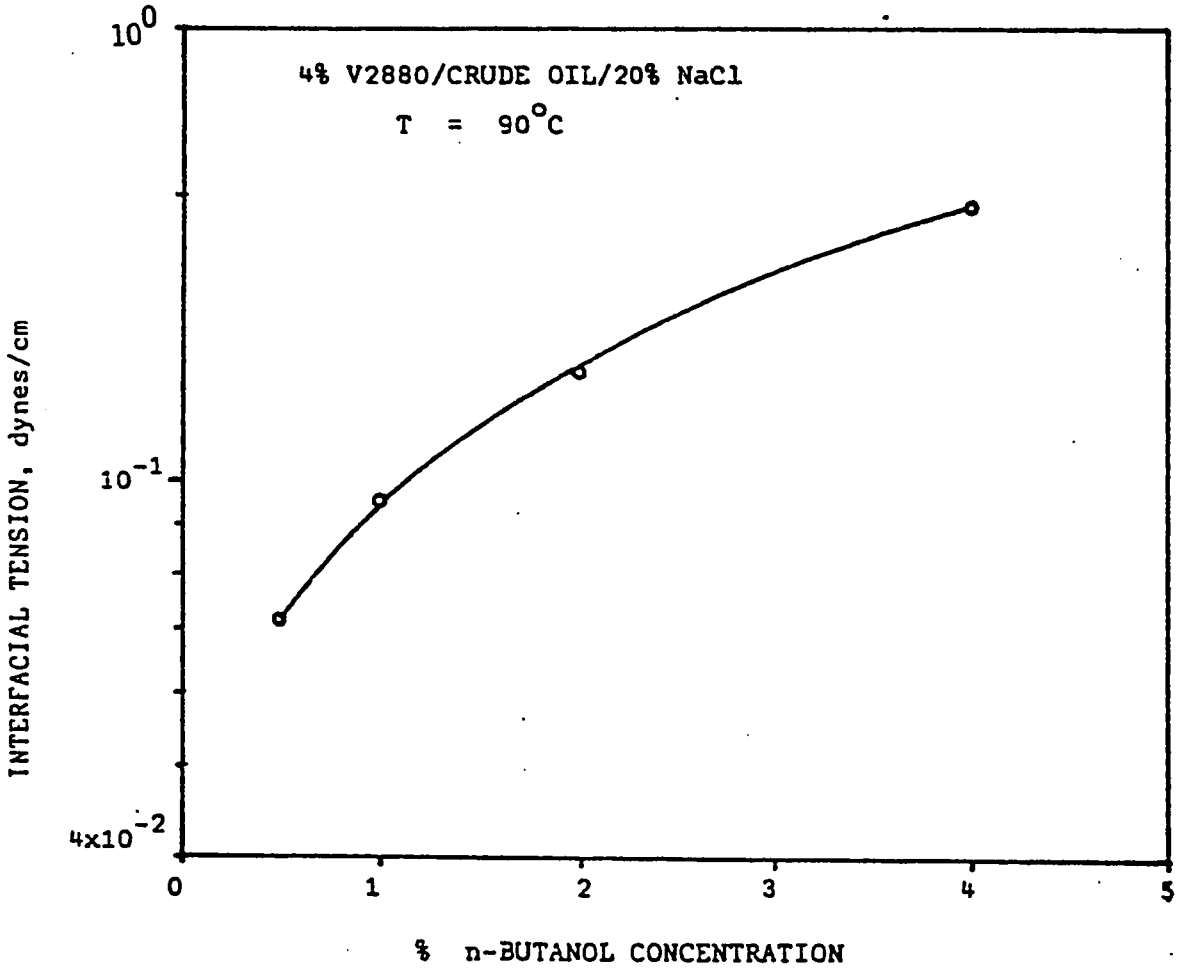

Fig. 15: Variation of IFT with Alcohol Concentration.

For each system therefore the amount of alcohol should be monitored for an effective IFT reduction.

Effect of Surfactant Concentration on IFT of V2880/Crude Oil System

The amount of surfactant incorporated into a micellar slug is limited by economics and other design conditions. Dependence of IFT on surfactant concentration provides a useful means to determine an optimum injection formulation. The effect of surfactant concentration on the interfacial activity of a slug, was therefore studied at constant salinity while varying only the surfactant concentration. IFT behavior of varying surfactant levels for V2880/crude oil system is illustrated in Fig. 16. V2880 apparently exhibits a minimum IFT at 2% surfactant concentration. Shah (8) observed two regions of ultra-low IFT in studying TRS10-410 with dodecane. At 0.1% TRS10-410 concentration, a minimum in IFT corresponding to the CMC was obtained followed by another minimum at 4.5% surfactant concentration. It should be noted that in our system the minimum corresponds to the latter one as no measurements were carried out in the vicinity of CMC.

Interfacial Tension Behavior of B1083 with Crude Oil (salinity scan)

The surfactant B1083 has an ethoxylation number of 15, as opposed

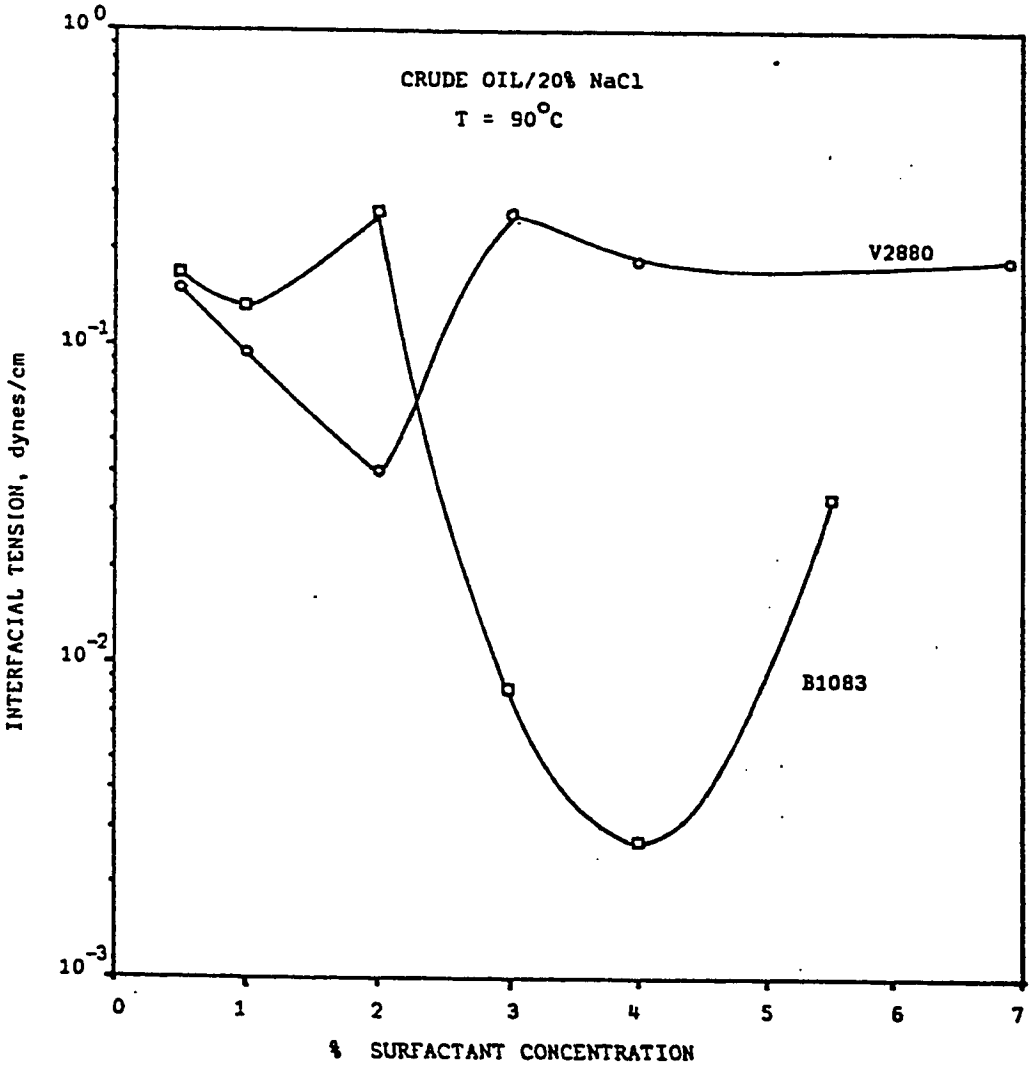

Fig 16: Effect of Surfactant Concentration on IFT for Two Different Surfactants.

to 8, for V2880 studied earlier. Therefore, this surfactant (B1083) is expected to exhibit more salt tolerance compared to V2880.

The effect of salinity on the interfacial tension of B1083 is presented in Fig. 17. The interfacial tensions between the oil and the aqueous phases exhibit two minima, one at about 14% NaCl concentration and the other at approximately 20% salinity. Again the first minimum corresponds to the classical three-phase region in Winsor's type III diagram. The solutions in the secondary optimal salinity region also exhibit three phases with a distinct middle phase similar to those obtained in the primary optimal salinity region. It should be emphasized that the presence of the secondary optimal salinity at 90°C is extremely important for high-salinity and high-temperature reservoirs as it can be favorably utilized in the design of appropriate surfactants.

As observed by the Texas group (22) ethoxylated surfactants have high electrolyte tolerance even in the presence of divalent ions. Due to their tendency to form liquid crystals at low temperatures, considerable amount of alcohol as cosurfactant may be required to form microemulsions. Liquid crystal formation has however been avoided by conducting this study at 90°C .

Interfacial Tension Behavior of B1083/Dodecane System (salinity scan)

Data obtained in previous sections for V2880 showed that crude oil

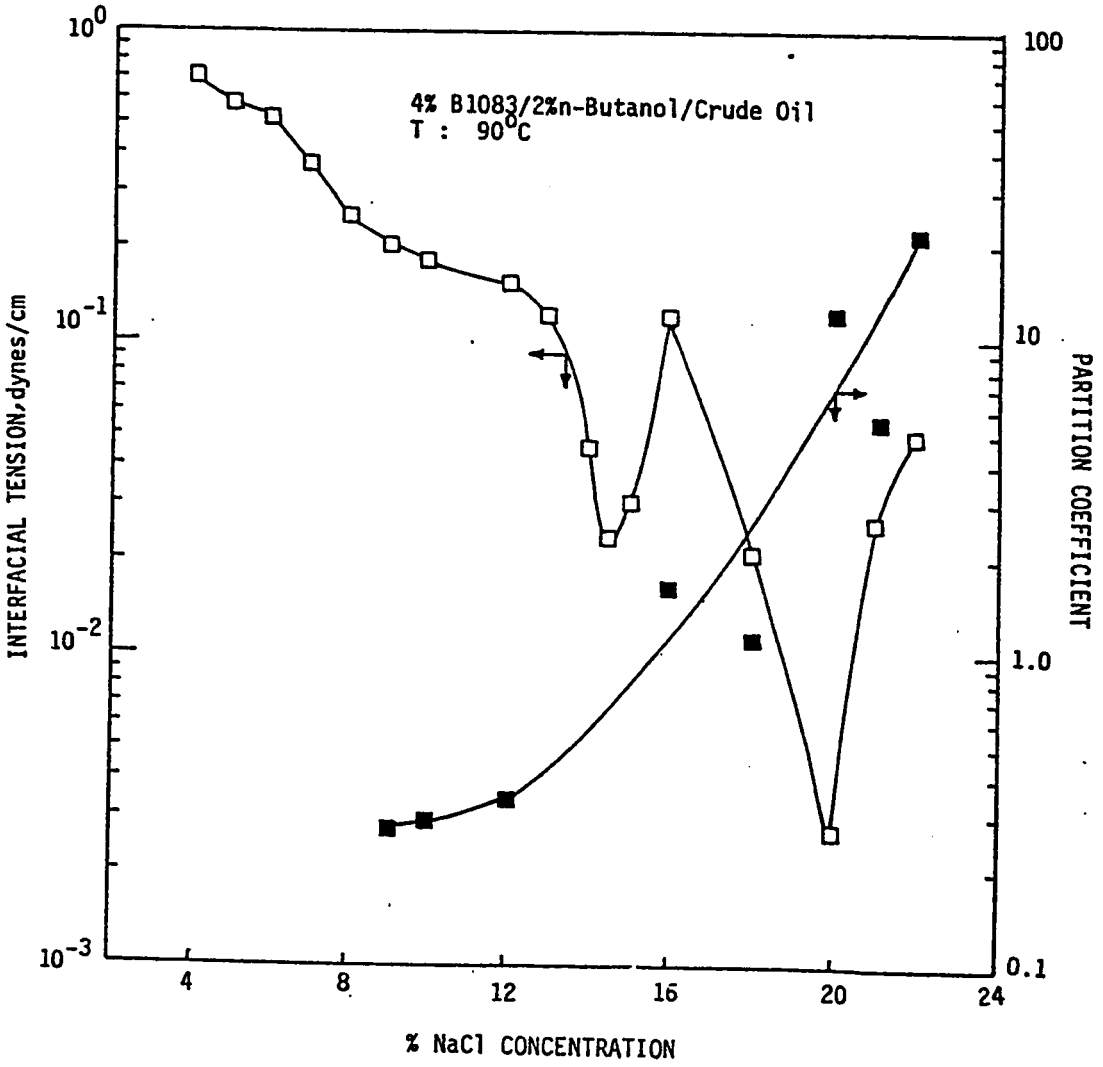

Fig. 17: Effect of Salinity on IFT and Partition Coefficient of B1083/Crude Oil Systems.

and Dodecane exhibit similar IFT behavior. A set of experiments with B1083 was further designed to test this effect of crude oil and dodecane on IFT. All other experimental conditions were kept constant except the change in oleic phase. Examination of the data shown in Fig. 18 clearly reveals that, similar to the crude oil, the alkene also produces two minima. The first minimum occurring at 12% salinity yields unacceptably high IFT values for EOR. The second minimum attained at 22% salinity generated reasonably low IFT values for good oil recovery purposes.

Comparison of V2880 and B1083 with dodecane clearly shows that the optimal salinities have shifted from 8% to 12% and from 14% to 22% respectively. This behavior is in agreement with the surface activity of the respective surfactants. A similar trend was also obtained in the presence of crude oil (see Figures 13 and 17). It is worth noting that the IFT's recorded at the two minima are higher in the dodecane system than in the crude oil system.

More importantly, the data obtained with B1083 clearly demonstrate that the secondary optimal salinity is not an artifice. In fact, the interfacial tensions measured at the secondary optimal salinity were found to be even lower than those obtained at the primary optimal salinity (see Figs. 17 and 18). Thus the existence of the secondary optimal salinity seems to be universal for at least ethoxylated sulfonates of varying ethoxylation numbers irrespective of alkene type.

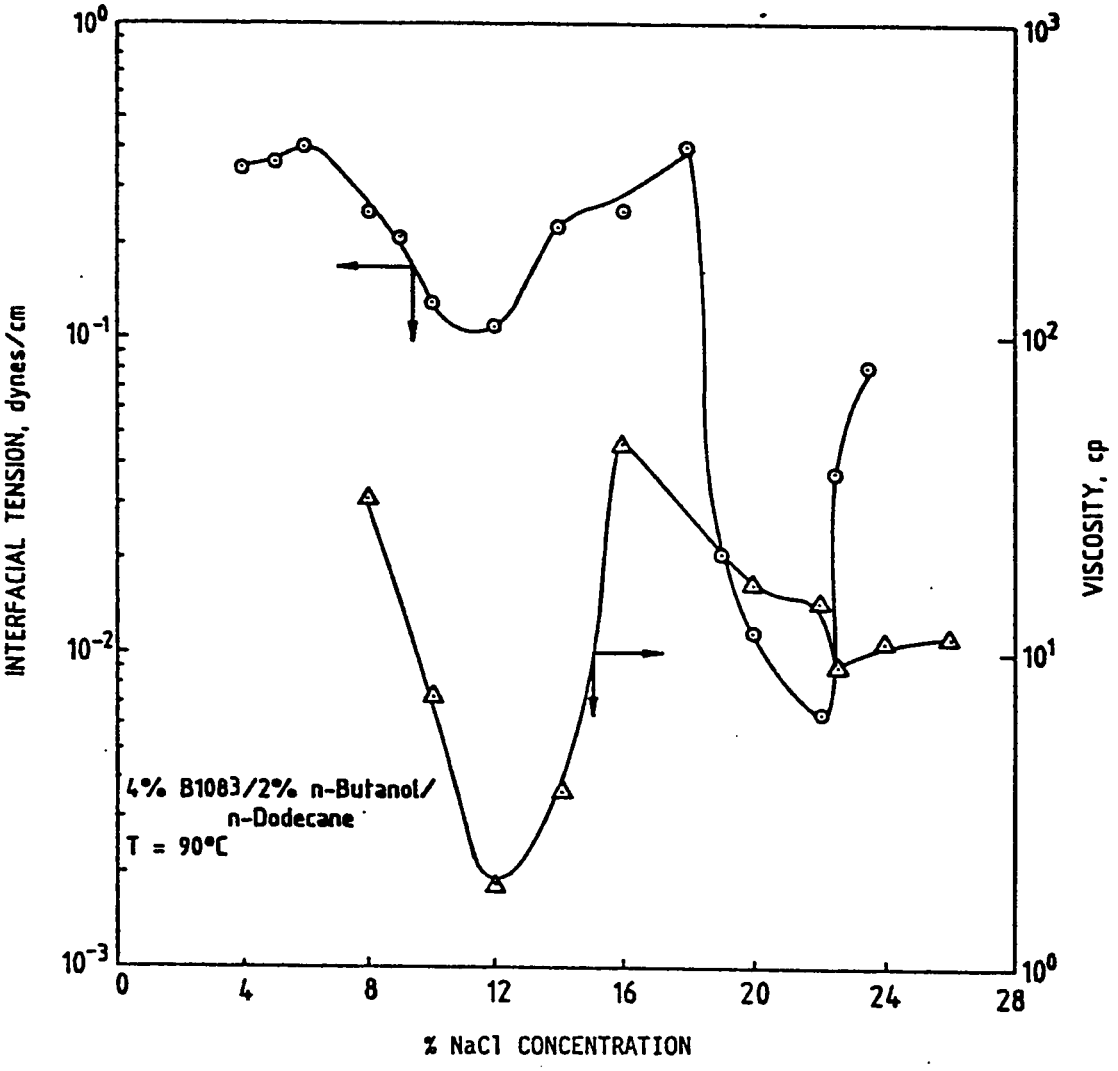

Fig. 18: Effect of Salinity on IFT and Middle Phase Viscosity in B1083/n-Dodecane System.

Interestingly, the viscosity of the middle phases generated minimuma at salinities corresponding to approximately the primary and secondary optimal salinities as shown in Fig. 18.

Effect of Surfactant Concentration on Interfacial Tension of B1083/Crude and B1083/Dodecane Systems

The dependence of IFT on B1083 concentration was studied by varying the surfactant concentration in a crude oil system. Results from this experiment are presented in Fig. 16. For the purpose of comparison the corresponding graph for the previously studied surfactant V2880 is also presented on the same figure. Both surfactants are found to exhibit a minimum IFT at a particular surfactant concentration. While V2880 yields a minimum at 2% surfactant concentration, B1083 shows the minimum IFT at 4% surfactant concentration. This trend is in accord with their respective surface activities. As V2880 contains less number of ethoxy groups, its surface activity is expected to be higher than that of B1083.

Comparison of the IFT behavior of B1083 with crude oil and dodecane exhibited a striking difference as illustrated in Fig. 19. While the IFT vs. concentration profile in the presence of crude oil generated a minimum at 4% B1083 concentration (Fig. 16) no such minimum was observed with dodecane (Fig. 19). Dodecane produced two distinct regions: At low concentrations (below 4%) the decrease in IFT is drastic whereas at higher surfactant concentrations the IFT seems to level off.

The foregoing discussion reveals that the EACN concept of standardizing a crude oil with an equivalent pure alkene may not agree

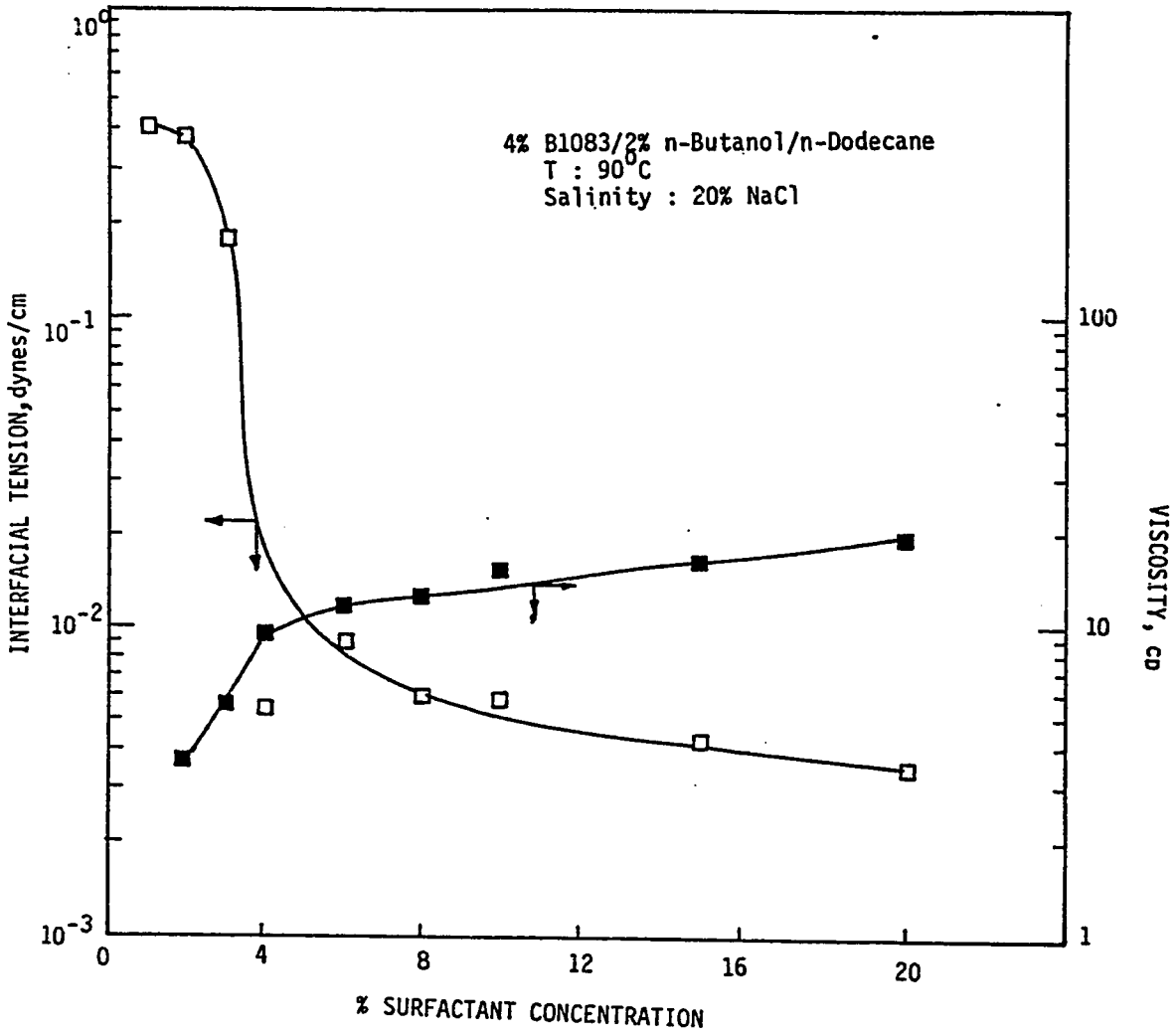

Fig. 19: Effect of Surfactant Concentration on IFT and Middle Phase Viscosity in B1083/n-Dodecane System.

under every condition. For instance, the coincidence of IFT vs. salinity for both crude oil and dodecane may not identify the actual EACN of a crude oil. Experiments under various conditions should be conducted to verify this inference.

The viscosity of the middle phase microemulsion in the presence of dodecane was also measured for B1083. Figure 19 displays the trend of viscosity with increasing surfactant concentration. Apparently, the viscosity data also follow a trend similar to the IFT behavior discussed above; the viscosity increases drastically at low surfactant concentrations whereas at higher concentrations, the increase is more gradual and eventually flattens out beyond a certain concentration.

The IFT data obtained with dodecane are analogous to the findings of Healy and Reed (4). In their study of the MEAC12OXS/TAA system, they observed that the optimal salinity corresponding to the minimum IFT is relatively constant over a wide range of surfactant concentration, above 3%. This implies that surfactant concentration ceases to influence IFT reduction after a certain point, for particular oil systems. In our system, the presence of minimum may be attributed to the impurities in the crude oil.

Effect of Alcohol Concentration on Interfacial Tension of B1083/ Crude Oil and B1083/Dodecane

As alcohol acts as a cosurfactant and aids the formation of microemulsion, its effect on IFT was investigated using two different oil systems. For the purpose of comparison, interfacial tensions were plotted against n-butanol concentration for the two systems investigated, (See Fig. 20). Alcohol concentration is observed to influence interfacial activity in a similar fashion for both the crude oil and dodecane. For the two systems it is observed that IFT decreases with increasing alcohol concentration. Interestingly, a broad minimum in IFT is achieved at the same alcohol concentration for both systems; above 2% alcohol concentration, interfacial tension is found to increase in both systems.

The results of this experiment indicate that, despite the major compositional differences, both oils respond to alcohol in a similar way. Another striking feature is that the IFT recorded for dodecane is higher than that for crude oil at all alcohol concentrations. This may be explained by the fact that while dodecane constitutes only one type molecule, the crude oil contains numerous components that can lead to the creation of a critical point. Particularly, the presence of higher molecular weight components in crude oil can induce such higher surface activity.

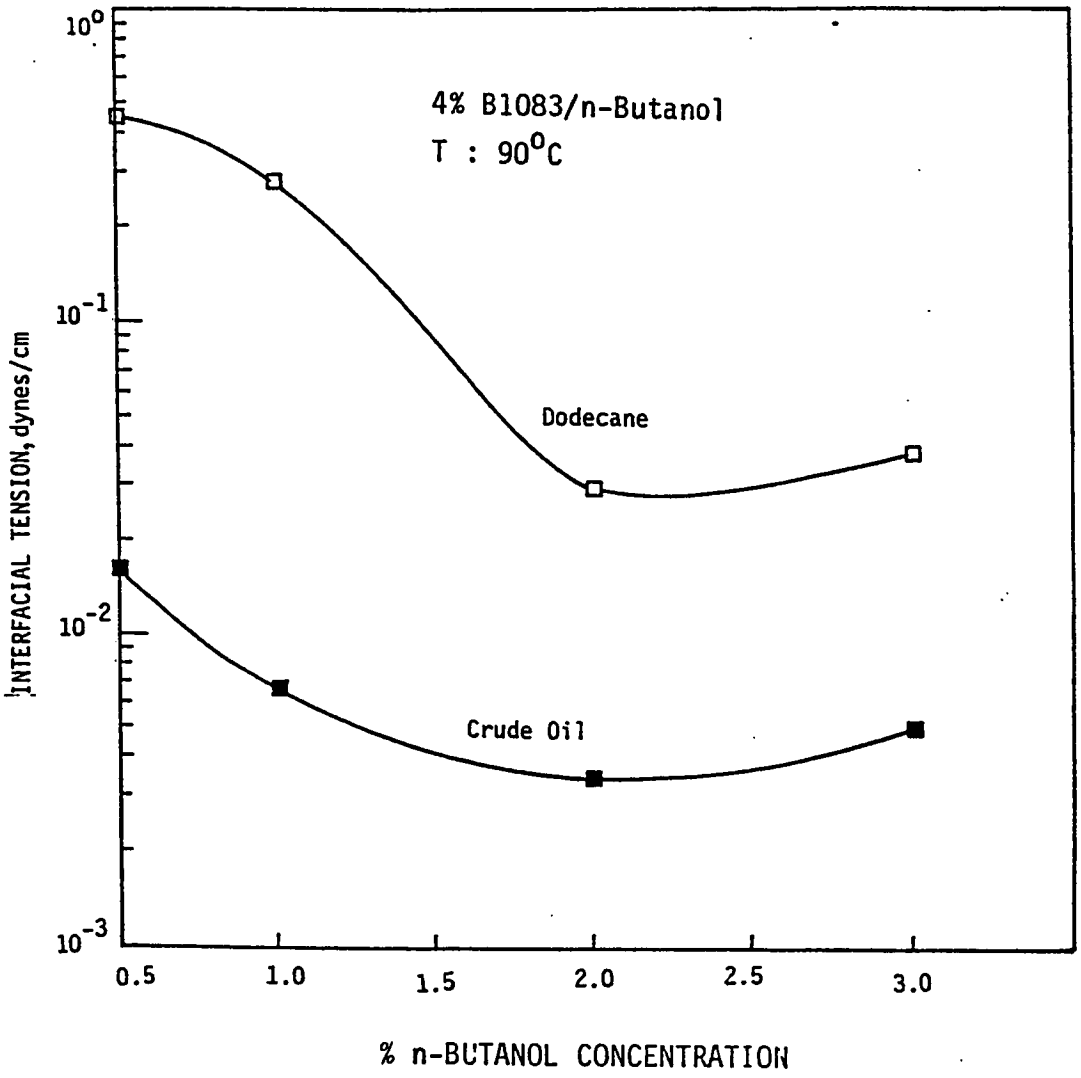

Fig. 20: Effect of Alcohol Concentration on IFT of B1083 and Two Different Oils.

The effect of alcohol on interfacial activity can be explained by the formation of microemulsion. Figure 21 shows the formation of various structures in surfactant solution upon increasing the surfactant concentration and adding alcohol.

It is shown in this diagram that with the addition of alcohol and oil, hexagonal packing of water cylinders are converted to microemulsion . The formation of middle phase microemulsion is markedly dependent on the amount of alcohol incorporated into the surfactant exemplifying the major role of alcohol in phase behavior studies. As noted by Salager (30) the middle phase microemulsion formed with TRS10-80 and sec-butanol with nonane, decreases progressively as the alcohol concentration is increased.

Alcohol Chainlength Effects on IFT of B1083 and Dodecane.

Since it has been established that alcohol affects formation of microemulsion this experiment was designed to show how variation of alcohol chainlength can influence the level of interfacial activity. Alcohols with carbon chainlength of 3 to 6 were used, including a control sample without any alcohol. A plot of interfacial tension against alcohol chainlength presented in Fig. 22 shows that IFT decreases continuously with increasing chainlength.

These data may imply that higher chainlength alcohols are more

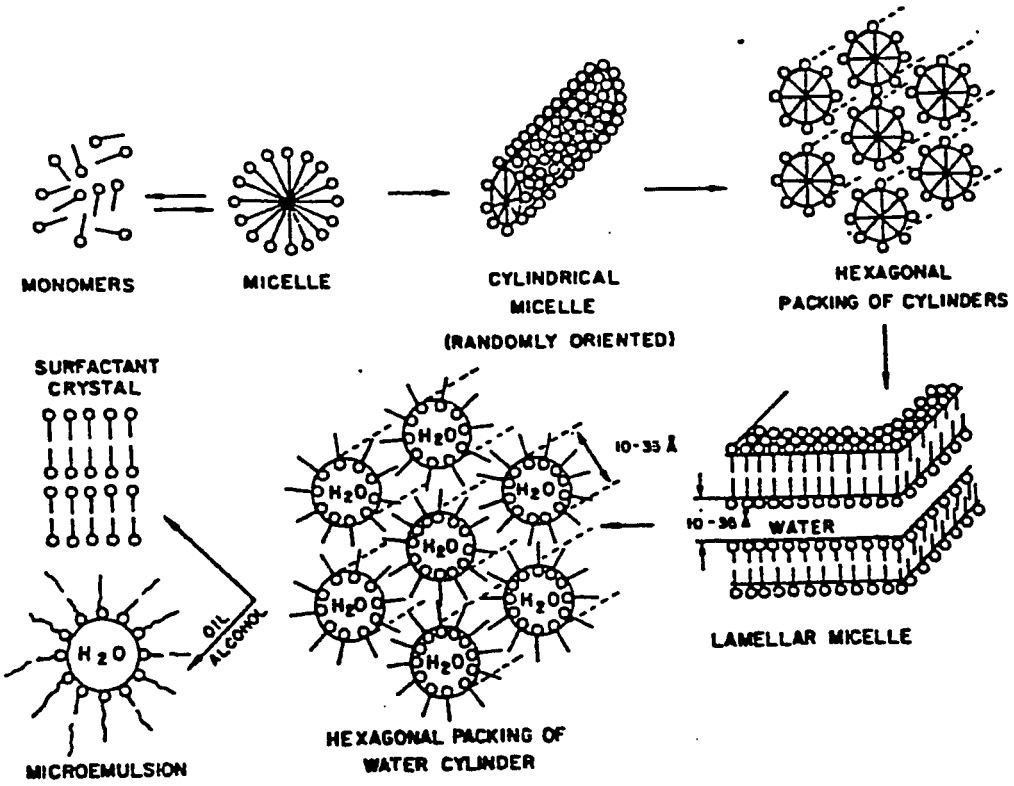

Fig. 21: Structure Formation in Surfactant Solution. (Ref. 32)

suitable but they pose a number of problems. For example as noted by Hsieh (6), higher chainlength alcohols give good IFT reduction only at low salinities. Lower chainlength alcohols not only withstand higher salinities but also cause lesser adsorption on reservoir rocks. It is also wellknown that higher chainlength alcohols are less soluble than those with lower chainlengths.

However, higher chainlength alcohols give phase behavior favorable to the surfactant slug designer as the slug proceeds through type I - III - II. As a compromise therefore, alcohols with chainlength closer to the lower scale of higher chainlength (C 4 and upward) tend to be used. Butanol has therefore been used in much of this study. Alcohols with chainlength lower than butanol are to be avoided because they cause phase behavior to change from type II - III - I which is undesirable (30). Moreover, as depicted on Fig. 22 they give intolerably high interfacial tensions.

The length of the alkyl chain of surfactants, alkanols, and alkenes has been found to influence the properties and structure of the interfaces in a microemulsion system. Shah and his coworkers (46) proposed a concept of structural "chainlength compatibility" effect. This concept expresses that maximum solubilization of water in the microemulsion would occur due to maximum cohesive interaction between the paraffinic chains when

$$l_a + l_o = l_s \qquad (4.2)$$

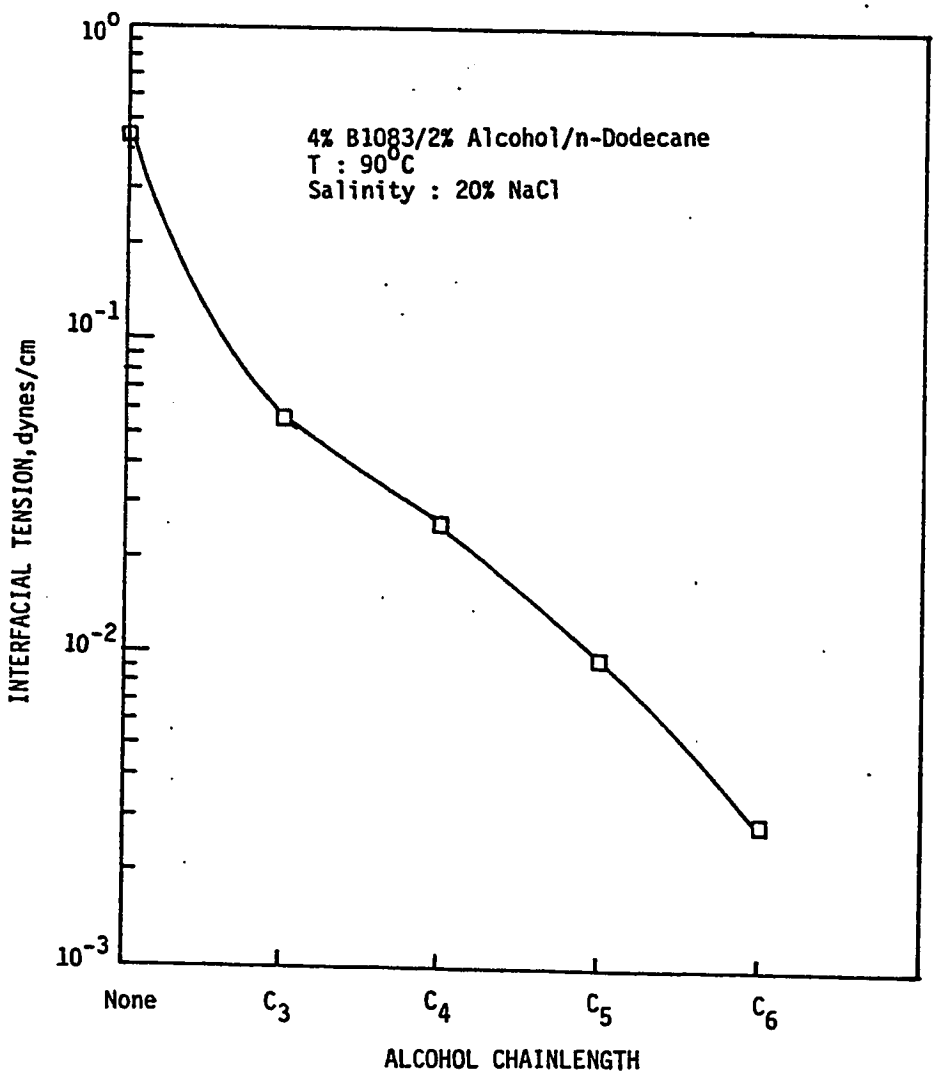

Fig. 22: Effect of Alcohol Chainlength on IFT of B1083/n-Dodecane System.

where l_a, l_o and l_s respectively denote alcohol, oil and surfactant chainlength. Shah et al (46) suggested that the matching of the chains would cause no dangling terminal groups and thus lead to improved order of the interfacial structure. However, Shah et al (47) in a recent study refuted this idea of molecular structural compatibility. Their measurements indicated that water solubilization limit is independent of the molecular structure of the oil, i.e. equation (4.2) is not necessarily true. More crucial are the bulk properties such as the surfactant and alcohol activity in the oil.

The above discussion on the alkyl chain compatibility clearly shows that for a complete design of micellar fluids a single rule of thumb does not exist yet. One should rather examine a set of properties such as IFT, solubilization parameters, partition coefficients and oil recovery tests to formulate the conducive conditions.

4.4 Ternary Diagram Representations

Ternary representation for B1083/Dodecane system at 12% NaCl.

The preceding discussion on B1083 indicated that B1083 exhibits the primary minimum at 90°C and 12% NaCl concentration. Therefore, this salinity level was selected for ternary representation studies. The surfactant concentration was kept constant at 4% while the water to oil

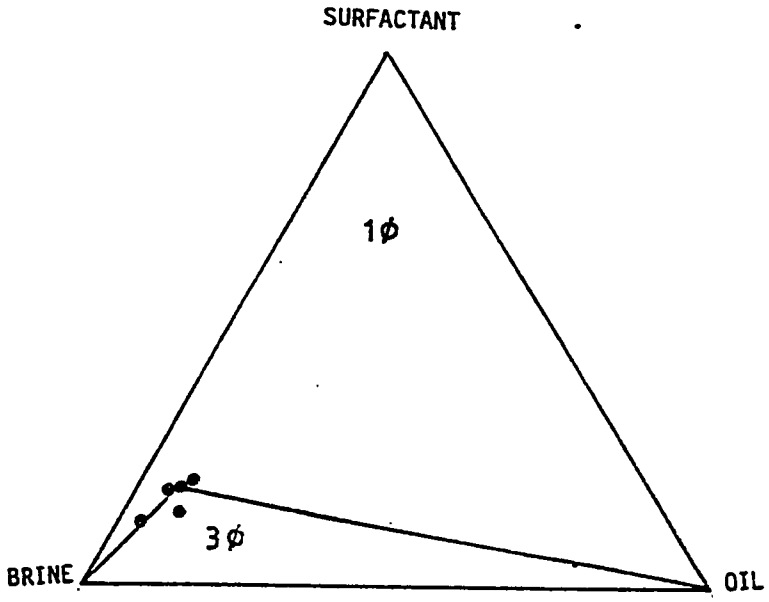

Fig. 23: Ternary Diagram Representation for 4% B1083/2%n-Butanol/ n-Dodecane System at 90°C and 12% NaCl.

ratio was varied. Three phases were observed in all tubes with WOR exceeding 1.0. For samples with WOR less than unity the formation of a foamy layer between the aqueous and oleic layers was observed. Analysis of the samples showed neglegible amounts of surfactant both in the aqueous and oleic phases. Almost all the surfactant was found to accumulate in the middle phase.

Figure 23 shows the nature of the three phase "triangle" with this formulation. The composition of the middle phase microemulsion represented by circles was found to scatter slightly. This is in agreement with the finding of Healy and Reed (4). They showed that for real systems, the composition of the middle phase microemulsion is not invariant but scatters, and in some cases falls on a locus. The skewness of the three phase regions in Fig. 23 demonstrates that the salinity level is less than optimal.

The bottom tie line separating the three phase region from the two phase region below was located from the sample with excessive surfactant partitioning into the brine in the presence of a middle phase microemulsion. The slope of this bottom tie line also confirms that the salinity level used here, 12%, is between the type II$^-$ and type III medium.

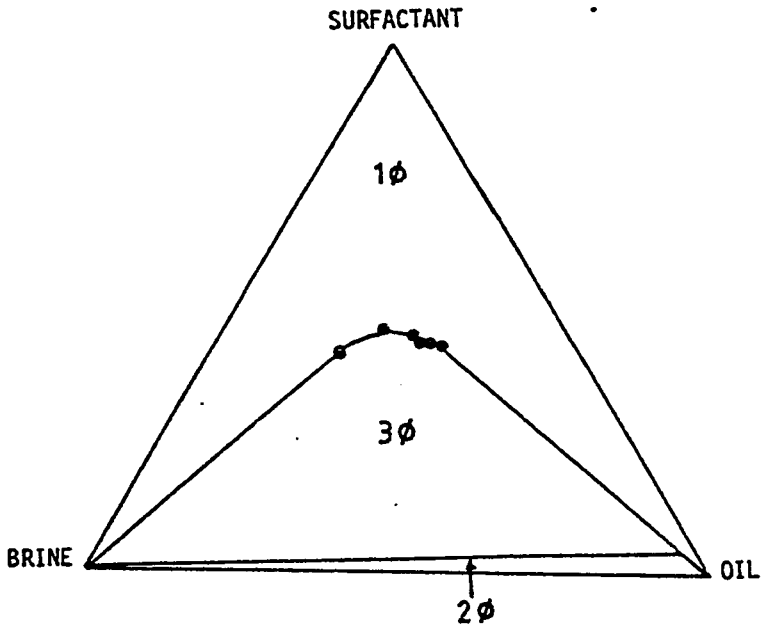

Fig. 24: Ternary Diagram Representation for 4% B1083/2%n-Butanol/ n-Dodecane System at 90°C and 20% NaCl.

Ternary Representation of B1083/Dodecane System at 20% NaCl

Since our target salinity is 20% and also the IFT measurements showed that 20% salinity is close to the secondary optimal salinity (see Fig. 18), ternary representation studies were therefore carried out with this salinity. The surfactant concentration was again kept constant at 4%. The water-to-oil ratio was varied to cover a wide range of aqueous/oleic combinations. The formation of three phases was observed in all tubes with WOR greater than 0.5. The presence of foam formation observed at lower salinities was absent at this salinity level.

The different phase regimes obtainable with this formulation are shown in Fig. 24. As observed earlier, the composition of the middle phase microemulsion is a locus in this representation. More importantly, the composition points are more centralized on the ternary diagram. The absence of skewness of the three phase region demonstrates that 20% salinity is the medium salinity. Nelson (27) pointed out that at the medium salinity the three phase "triangle" is more or less isosceles. The two-phase region below the "triangle" was located by observing large surfactant partitioning into the oil in a tube having three phases (30).

Ternary Representation of B1083/Dodecane System at 24% Salinity

Above the secondary optimal salinity another region of low IFT

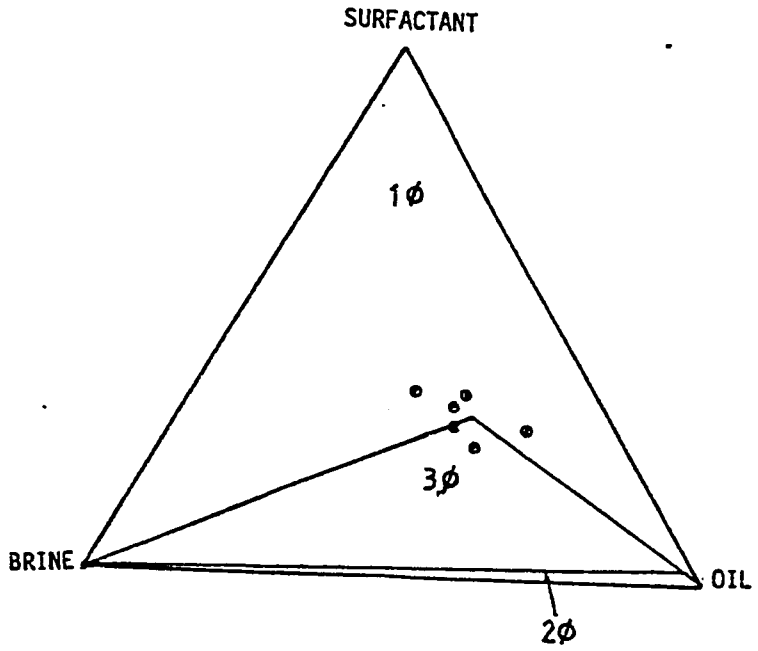

Fig. 25: Ternary Diagram Representation for 4% B1083/2%n-Butanol/ n-Dodecane System at 90°C and 24% NaCl.

occurred in the vicinity of 24% NaCl. Experiments similar to the one described above were also conducted at this salinity level. The formation of three phases was observed in all the water-oil ratios scanned except one. Foam formation was also not observed in this experiment. As with the other experiments, surfactant partitioning into the excess brine and oleic phases was negligible.

Figure 25 shows the phase regimes given by this salinity level. It is observed that the three phase triangle is skewed to the right, implying this salinity level is above medium (27). Skewness to the right in this Figure reveals that more oil than water is contained in the middle phase microemulsion. The positive slope of the bottom tie line also suggests that this salinity level is between medium salinity and type II^+ regime.

Ternary Representation of B1083/Crude Oil System at 20% Salinity

At the target salinity of 20%, crude oil also produced rather low IFT in the salinity scan experiments. Therefore, phase behavior studies were conducted to map the different phase regimes. For all combinations of water to oil ratios, middle phase microemulsion was predominant. The delineation of the middle phase microemulsion was made by the use of ultraviolet light.

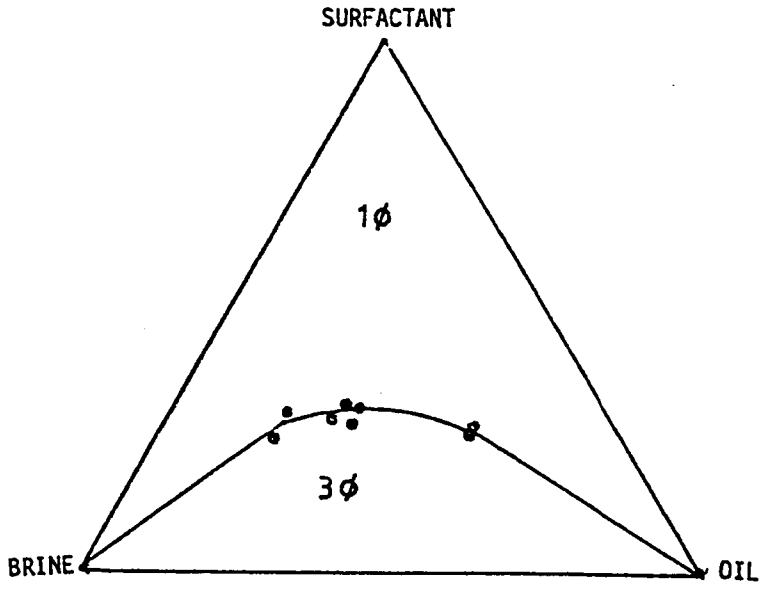

Fig. 26: Ternary Diagram Representation for 4% B1083/2%n-Butanol/ Crude Oil System at 90°C and 20% NaCl.

The compositions of the middle phase microemulsion are presented in Fig. 26. Similar to the other systems studied previously, the compositions fall on a locus instead of a single point. More strikingly the scatter in the crude oil plot is noticed to be wider than that of dodecane. This is indicative of the more heterogenous nature of crude oil. Pure systems tend to give less scattering of the middle phase microemulsion composition. The bottom tie line is not observed in the crude oil system because of the negligible surfactant partitioning into the lower and upper phases in all the samples considered. While the presence of the two phase region below the three phase triangle is observed in all systems, negligible surfactant partitioning makes the bottom tie line almost to coincide with the zero percent surfactant line.

By increasing surfactant concentration to 20% at 20% salinity, middle phase formation was observed at all water to oil ratios, similar to the behavior at lower surfactant concentrations. Analysis of the middle phase microemulsion showed an increased percentage of surfactant in the microemulsion at the expense of oil and water (see Fig. 27). While at 4% B1083 concentration the microemulsion composition averaged 40:32:27 water/surfactant/oil ratios, it was 10:75:15 at 20% concentration. It can therefore be said that at the high surfactant concentration of 20%, solubilization of both oil and water are drastically reduced. Beside economic considerations, this observation makes the use of high surfactant concentrations in micellar flooding unadvisable.

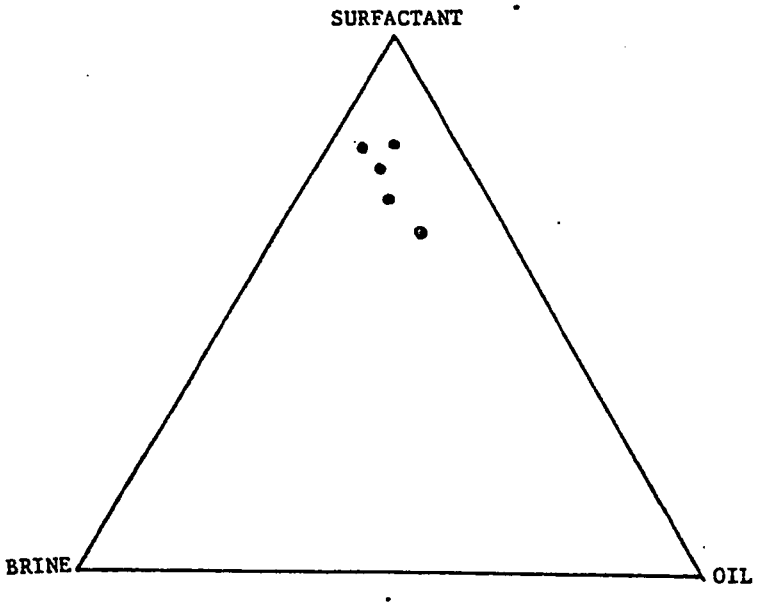

Fig. 27: Ternary Diagram Representation for 20% B1083/10% n-Butanol/Crude Oil System at 90°C and 20% NaCl.

It is important to recognize that for our target reservoir conditions of salinity and temperature, the solutions remain in the three phase region- the lowest IFT region- with widely varying water to oil ratios. This feature can facilitate the prediction of the phase behavior under actual field conditions.

CHAPTER 5

CHAPTER 5

SUMMARY AND CONCLUSIONS

The phase behavior of surfactants in the presence of a crude oil and an alkane was studied with a particular emphasis on the interfacial tensions between the different phases. Partition coefficients of the surfactants into oil and brine were also studied. A new finding of major importance, secondary optimal salinity is presented along with its governing mechanism. A slug composition is formulated for the harsh Saudi Arabian Limestone reservoirs. The following conclusions can be drawn:

1. Petroleum sulfonates are not salt tolerant and tend to give low optimal salinities. The IFT study of the petroleum sulfonate (TRS10-410) with crude oil both at low and high temperatures revealed its low salt tolerance.

2. The nonionic surfactant, Sapogenat T-150, gives intolerably high IFT and is not suitable for high-temperature and high-salinity reservoirs.

3. Ethoxylated sulfonates, however, are salt tolerant even at high temperatures and high salinities. The high optimal salinities obtained with these surfactants are particularly suitable for rather harsh reservoirs such as Saudi Arabian Limestone reservoirs.

4. Alcohol is an indispensable component in slug formulation of

ethoxylated sulfonates to obtain low IFT. Short chian alcohols are preferable to longer chain alcohols as the latter tend to be insoluble in brine.

5. In addition to the primary optimal salinity, this study has shown the existence of another region of low IFT (secondary optimal salinity) occurring at higher salinity levels. Even more importantly, this secondary optimal salinity region yields lower IFT's.This phenomenon is of considerable importance to slug design for high-temperature and high-salinity reservoirs.

6. The primary and secondary optimal salinties were found to shift to higher salinities with increasing ethoxylation number of the ethoxylated sulfonates. This is consistent with the surface activity of this group of surfactants and further confirms the reality of the secondary optimal salinity.

7. While the primary optimal salinity has been explained by the classical three phase formation and the occurrence of critical points, the secondary optimal salinity can be attributed to the formation of a thin interfacial layer between the excess phases.

8. For the target conditions of 20% salinity and 90°C, the ethoxylated sulfonate (B1083) produced low interfacial tensions for good oil recovery. In addition, the formation of three phases with this surfactant at the conditions of this study prevails over a wide range

of WOR.

9. Ternary representations with the ethoxylated sulfonate (B1083), EO=15 revealed that 20% salinity which corresponds to the secondary optimal salinity, produced a symmetric three phase 'triangle'. This implies that the salinity level of 20% gives good IFT lowering and efficient displacement.

CHAPTER 6

CHAPTER 6

RECOMMENDATIONS

1. The structure and mechanism of microemulsions formed at the primary and secondary optimal salinities need to be furhter studied.

2. Ethoxylated sulfonates with higher EON and also their mixtures should be investigated.

3. Different chain length alcohols may be tried as cosurfactants.

4. A synthetic brine of approximately the same constitution as reservoir brine may be used in phase behavior studies.

5. The interaction of ethoxylated sulfonates with mobility control agent (polymer) should be investigated.

REFERENCES

REFERENCES

1. Schulman, J.H, Stoeckenius, W. and Prince, L.M., "Mechanism of formation and structure of microemulsions by electron microscopy," J. Phys. Chem., 63, (1959) 1677.
2. Winsor, P.A., "Solvent properties of amphiphilic compounds," Butterworth's Scientific Publications, London, 1954.
3. Healy, R.N and Reed, R.L., "Physicochemical Aspects of Microemulsion Flooding," Soc. Pet. Eng. J.,(Oct. 1974) 491-501.
4. Healy, R.N and Reed, R.L., "Multiphase microemulsion systems," Soc. Pet. Eng. J.,(June 1976) 147-160.
5. Jones, S.C and Dreher, K.D., "Cosurfactants in micellar system used in Tertiary Oil Recovery,"Soc. Pet. Eng. J.,(June 1970) 161-167.
6. Hsieh,W.C. "Microemulsion stability and interfacial properties of surfactant formulations in relation to tertiary oil recovery," Ph.D Dissertation, University of Florida, 1977.
7. Vinatieri, J.E., "Correlation of emulsion stability with phase behavior in surfactant systems for tertiary oil recovery," Soc. Pet. Eng. J.,(Oct. 1980) 402-406.
8. Shah, D.O., "Fundamental aspects of surfactant/polymer flooding process," in the Proceedings of third European Symposium on Enhanced Oil Recovery, ed., Fayer, F.J.,UK, Sep., 1980.
9. Andrews, C.,Colley, N.M. and Thaver, R., "Preliminary studies of the phase behavior of some commercially available surfactants in

hydrocarbon-brine-mineral systems," in the Proceedings of third European Symposium on Enhanced Oil Recovery, ed., Fayer, F.J.,U.K, Sep. 1980.

10. Anderson, D.R.,Binder, M.S, Davis, H.T, Manning C.O.,and Scriven L.E. "Interfacial tension and phase behavior in surfactant-brine-oil systems," SPE Paper 5811, 1976.
11. Min, K.T.,and Lorenz, P.B. "The EACN of a crude oil: Variations with cosurfactants and water-oil ratio," in the Proceedings of third European Symposium on Enhanced Oil Recovery, ed.,Fayer, F.J., U.K, Sep. 1980.
12. Larson, R.G., "The influence of phase behavior on surfactant flooding," Soc. Pet. Eng. J.,(Dec.1979) 411-422.
13. Nelson, R.C.,"The effect of live-crude on phase behavior and oil recovery efficiency of surfactant flooding systems," Soc. Pet. Eng. J., (June 1983) 501-510.
14. Koukounis, C., Wade, W.H. and Schechter, R.S., "Phase partitioning of ionic and nonionic surfactant mixtures," Soc. Pet. Eng. J., (April 1983) 301-310.
15. Rossen, W.R. and Kohn, J.P.," Behavior of microemulsions under compression," Soc. Pet. Eng. J.,(Oct 1984) 536-544.
16. Bellocq, A.M, Biasi, J., Bothorel, P., Clin, B., Lalanne, P., Lemaire, B., Lemanceau, B. and Roux, D., "Microemulsions," Advances in Colloid and Interface Science, 20, (1984) 167-272.
17. Qutubuddin, S., Miller, C.A. and Fort, T. Jr., "Phase Behavior

of pH dependent microemulsions, "Journal of Colloid and Interface Science. Vol. 101, No. 1 (Sep. 1984) 46-58.

18. Nelson, R.C., "The salinity-requirement diagram - A useful tool in chemical flooding research and development," Soc. Pet. Eng J.,(April 1982) 259-270.

19. Graciaa, A., Fortney, L.N., Schechter, R.S., Wade, W.H., Yiv, S., "Criteria for structuring surfactants to maximize solubilization of oil and water: Part 1 - Commercial nonionics," Soc. Pet. Eng. J.,(October 1982) 737.

20. Barkat, Y., Fortney, L.N., Schechter, R.S., Wade, W.H., Yiu S., "Criteria for structuring surfactants to maximize solubilization of oil and water, Part II - Alkyl Benzene sodium sulphates," J. of Colloid and Interface Science, 92, (April 1983) 561-574.

21. Glover, C.J., Puerto, M.C., Maerker, J.M., Sardvik, E.L., "Surfactant phase behavior and retention in porous media," Soc. Pet. Eng. J.,(June 1979) 183-193.

22. Carmona, I., Schechter, R.S., Wade, W.H., Upali, W., "Ethoxylated oleyl sulfonates as model components for enhanced oil recovery," Soc. Pet. Eng. J.,(June 1985) 351-357.

23. Chou, S.I., Bae, J.H., "Phase behavior correlation for high-salinity surfactant formulations," SPE/DOE Paper 14913, Presented at the Fifth Symposium on Enhanced Oil Recovery, Tulsa, Oklahoma, (April 1986).

24. Smith, D.H., "Tricritical points and the design of high-salinity

surfactants for low-tension enhanced oil recovery," SPE/DOE Paper 14914, Presented at the Fifth Symposium on Enhanced Oil Recovery, Tulsa, Oklahoma, (April 1986).

25. Mitchell, D.J. and Ninham, B.W. "Micelles ,Vesicles and Macroemulsions," J. Chem. Soc. Faraday Trans. II, 77, (1981) 601-626.
26. Vinatieri, J.E. and Fleming, P.D., "Qualitative interpretation of phase volume behavior of multicomponent systems near critical points," AICh.EJ Vol. 25, (1979) 124.
27. Nelson, R.C. and Pope, G.A., "Phase relationships in chemical flooding," Soc. Pet. Eng. J.,(Oct. 1978) 325-338.
28. Cayais, J.L., Schechter, R.S., Nobe, W.H., "Modeling crude oils for low interfacial tension," Soc. Pet. Eng. J.,(Dec.1976) 351-357.
29. Verkruyse, L.A., Salter, S.J., "Potential use of nonionic surfactants in micellar flooding," SPE Paper 13574, Presented at the International Symposium on Oilfield and Geothermal Chemistry, Phoenix, Arizona, (April 1985).
30. Salager, J.L., "Physico-chemical properties of surfactant-water-oil mixtures: Phase behavior, microemulsion formation and interfacial tension," Ph.D. dissertation, University of Texas, Austin, (1977).
31. Cayais, J.L., Schechter, R.S., and Wade, W.H., "The Measurement of Low Interfacial Tension via the Spinning Drop Technique," ACS Symposuim Series, Number 8 , (1975) 243.

32. Shah, D.O.,Bansal, V.K.,Chan, K.and Hsieh, W.C., "The Structure, Formation and Phase-Inversion of Microemulsions," in Improved Oil Recovery by Surfactant and Polymer Flooding, Academic Press Inc., (1977).

33. Abe, M., Schechter, D., Schechter, R.S., Wade. W.H., Weerasooriya, V.,and Yiv, S., "Microemulsion Formation with Branched Tail Polyoxyethylene Sulfonate Surfactant," J. Colloid Interface Science,114, No.2, (Dec.1986) 342.

34. Fendler, J.H. and Fendler, E.J., "Catalysis in Micellar and Macromolecular Systems," Academic Press, 1975.

35. Becher, P., in Nonionic Surfactants, Schick, M.J., ed., Marcel Dakker, New York, (1967).

36. Nagakawa, "Solubilization of Nonionic Surfactants," in Nonionic Surfactants, Schick, M.J., ed., (1967) 558-603.

37. "Surfactant/Polymer Flooding of Saudi Limestone Reserviors," KASCT Progress Report No.2, AR-6-161, (Jan. 1986).

38. "Surfactant/Polymer Flooding of Saudi Limestone Reserviors," KASCT Progress Report No.4, AR-6-161, (Jan. 1987).

39. Lewis, S.J. Verkruyse, L.A. and Salter, S.J., "Selection of Nonionic Surfactants for Minimized Adsorption and Maximized Solubilization," Presented at SPE/DOE Symposium, SPE paper 14910,(April 1986), Tulsa.

40. Puerto, M.C. and Reed, R.L., "A Three-Parameter Representation of Surfactant-Oil-Brine Interaction," Soc. Petrol.Eng.J.,(August

1983) 669-682.

41. Koukounis, C.,Wade, W.H.and Schechter, R.S., "Phase Partitioning of Ionic and Nonionic Mixtures," Soc. Pet. Eng. J., (April 1983) 301.

42. Huh, C., "Interfacial Tension and Solubilization Ability of a Microemulsion Phase That Coexists with Oil and Brine", J.Colloid Interface Sci., 97, (1984) 201.

43. Healy, R.N.and Reed R.L.,"Some Physico-Chemical Aspects of Microemulsion Flooding," D.O. Shah and R.S. Schechter, eds., Academic Press, (1977) 383.

44. Seeto, Y., Piug, J.E., Scriven, L.E. and Davis, H.T., "Interfacial Tensions in Systems of Three Liquid Phases", J. Colloid Interface Sci., 96, (Dec. 1983) 360.

45. Fleming, P.D.and Vinatieri.J.E., "The Role of Critical Phenomena in Oil Recovery Systems Employing Surfactants", J.Colloid Interface Sci., 81, (1981) 319.

46. Bansal, V.K., Shah, D.O., and O'Connell, J.P., J. Colloid Interface Sci., 75, (1980) 462.

47. Leung, R., Shah, D.O.,and O'Connell, J.P., "Alkyl Chainlength Compatibility and Solubilization in Water-in-Oil Microemulsions," J. Colloid Interface Sci., 111,(1986) 286.

48. Akstinat,M.H., "Surfactants for EOR Processes in High-Salinity Systems," in Enhanced Oil Recovery, Developments in Petroleum Sci. 13, Ed., Fayers, F.J., (1981) 43-62.

49. Gulden, W., " The Industrial availability of Surfactants with Special Emphasis on EOR," Hoechst Internal Report, 1985.

50. Ahmed S., " Adsorption of Surfactants on Saudi Arabian Limestone Reservoirs," M.S. Thessis , KFUPM, Dhahran, Saudi Arabia, (1987).

APPENDIX A

Appendix A1 : Properties of Surfactants Used

Properties	Petroleum Sulfonate	Ethoxylated Sulfonates		Nonionic Surfactant
Brand Name	TRS10-410	V2880	B1083	T-150
Appearance at 25°C	Brownish liquid	Yellowish liquid	Yellowish liquid	Yellowish paste
Ethoxylation No.	--	8	15	15
Molecular Weight	420	720	1028	1058
% Active ingredient	62	30.1	21.4	100
% Solid Content	--	43.4	39.8	--
% Mineral Oil	33	--	--	--
% Salt Content	0.7	4	5	--
% Water Content	4.2	56.6	60.2	--
Density @ 25°C (g/cc)	--	1.05	1.07	1.08
Solubility @ 80°C	--	20%	20%	--
CMC (g/l)	--	0.21	0.43	0.17

Appendix A2 : Properties of Alcohols Used as Cosurfactants

Alcohol	Specific Gravity	Molecular Weight	Flash Point	Formula
Propanol	0.804	60.1	24°C	$CH_3(CH_2)_2OH$
Butanol	0.810	74.12	43°C	$CH_3(CH_2)_3OH$
Pentanol	0.812	88.15	38°C	$CH_3(CH_2)_4OH$
Hexanol	0.818	102.18	74°C	$CH_3(CH_2)_5OH$

Appendix A3: Calibration Curve for Two-Phase Titration of B1083

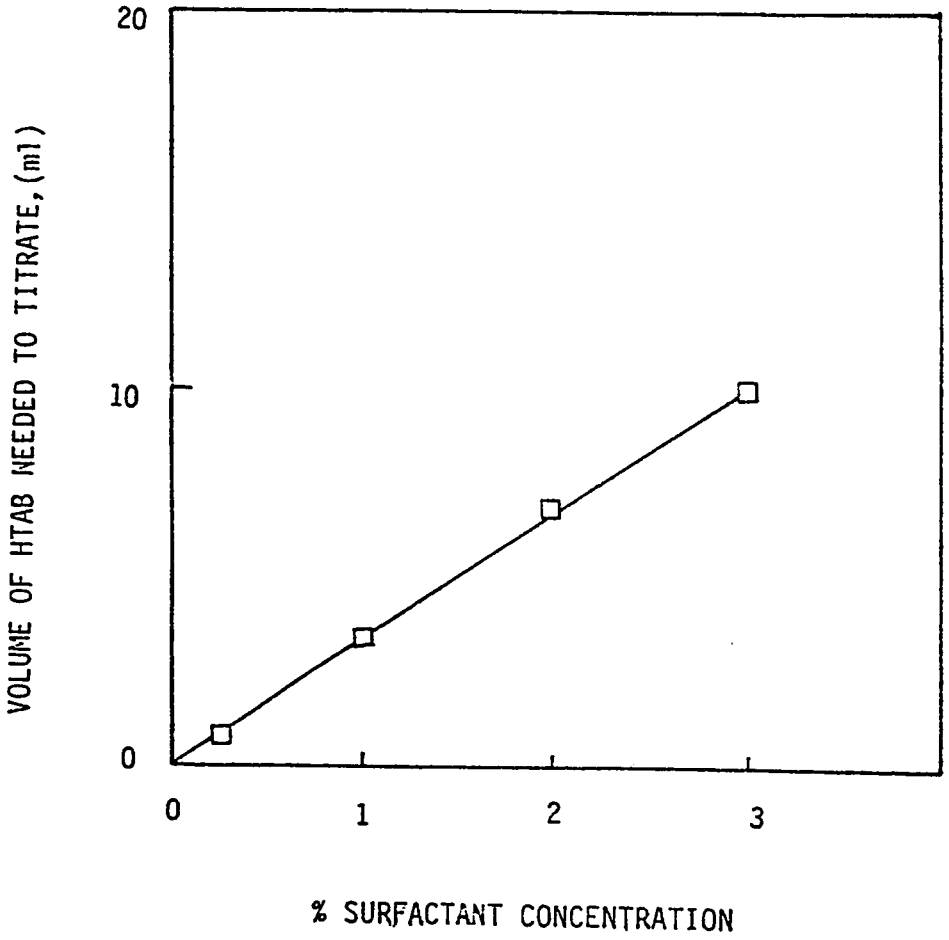

Appendix A4 : Table of Constants for Low Shear Viscometer.

D, τ UND η-TABELLE ZU LOW SHEAR 30, REPRAESENTATIVE WERTE

D, τ AND η-VALUES TABLE FOR LOW SHEAR 30, REPRESENTATIVE VALUES

Stufe / Step	η_{rep} [mPa.s] Range 1	Range 2	Range 3	Range 4	Range 5	D_{rep} [s^{-1}]	n [min^{-1}]
1	2,99	14,93	74,7	373	1867	0,01607	0,01332
2	2,20	10,99	54,9	275	1373	0,0219	0,01811
3	1,616	8,08	40,4	202	1010	0,0297	0,0246
4	1,189	5,95	29,7	148,6	743	0,0404	0,0335
5	0,875	4,37	21,9	109,3	547	0,0549	0,0455
6	0,643	3,22	16,09	80,4	402	0,0746	0,0618
7	0,463	2,37	11,83	59,2	296	0,1015	0,0841
8	0,348	1,741	8,71	43,5	218	0,1379	0,1143
9	0,256	1,281	6,40	32,0	160,1	0,1874	0,1553
10	0,1885	0,942	4,71	23,6	117,8	0,255	0,211
11	0,1386	0,693	3,47	17,33	86,6	0,346	0,287
12	0,1020	0,510	2,55	12,75	63,7	0,471	0,390
13	0,075	0,375	1,876	9,38	46,9	0,639	0,530
14	0,0552	0,276	1,380	6,90	34,5	0,870	0,721
15	0,0406	0,203	1,015	5,08	25,4	1,182	0,980
16	0,0299	0,1493	0,747	3,73	18,67	1,607	1,332
17	0,0220	0,1099	0,549	2,75	13,73	2,19	1,811
18	0,01616	0,0808	0,404	2,02	10,10	2,97	2,46
19	0,01189	0,0595	0,297	1,486	7,43	4,04	3,35
20	0,00875	0,0437	0,219	1,093	5,47	5,49	4,55
21	0,00643	0,0322	0,1609	0,804	4,02	7,46	6,18
22	0,00473	0,0237	0,1183	0,592	2,96	10,15	8,41
23	0,00348	0,01741	0,0871	0,435	2,18	13,79	11,43
24	0,00256	0,01281	0,0640	0,320	1,601	18,74	15,53
25	0,001885	0,00942	0,0471	0,236	1,178	25,5	21,1
26	0,001386	0,00693	0,0347	0,1733	0,866	34,6	28,7
27	0,001020	0,00510	0,0255	0,1275	0,637	47,1	39,0
28	0,000750	0,00375	0,01876	0,0938	0,469	63,9	53,0
29	0,000552	0,00276	0,01380	0,0690	0,345	87,0	72,1
30	0,000406	0,00203	0,01015	0,0508	0,254	118,2	98,0
τ_{rep} [mPa]	0,0480	0,240	1,201	6,00	30,0		

$K_{rep} = 0,9200$

$$\frac{\tau_{rep}}{K_{rep}} = \tau_i \qquad \frac{D_{rep}}{K_{rep}} = D_i$$

$$D_{rep} = 1,207 \cdot n$$

$$LS\ 30^{MB\text{-}LS\ 1}_{MK\text{-}LS\ 1}$$

APPENDIX B

Table 1 : Effect of Salinity on IFT of TRS10-410/Dodecane System

Surfactant :	4% TRS10-410	Alcohol :	2% n-Butanol
Temperature :	26°C	Oil :	Dodecane

Salinity %NaCl	IFT dynes/cm	Partition Coefficient
0.55	0.160	---
1.05	0.026	0.015
1.2	0.0076	0.04
1.3	0.0016	1.2
1.45	0.025	2.5
1.6	0.450	5.5
1.85	---	15.0

* Oil/microemulsion ** Microemulsion/aqueous

Table 2 : Effect of Salinity on IFT of TRS10-410/Crude Oil System

Surfactant : 4% TRS10-410 Alcohol : 2% n-Butanol

Temperature : 26°C Oil : Crude Oil

Salinity %NaCl	Drop Width 0.0001 cm	Spinning Rate(ms/rev)	Refractive Index	$\Delta\rho$ g/cc	IFT dynes/cm
0.5	293	8.50	1.3431	0.144	0.0138
1.0	107	8.51	1.3356	0.1268	0.00111
1.2	200	8.55	1.3361	0.1238	0.00701
1.3	179	8.56	1.3364	0.1196	0.00484
1.4	174	8.57	1.3366	0.1228	0.00460
1.5	197	8.55	1.3364	0.1308	0.00707
1.6	248	8.49	1.3366	0.1398	0.0153
1.7	266	8.48	1.3372	0.1238	0.0167
3.0	410	8.51	1.3391	0.1599	0.782
5.0	531	8.60	1.3425	0.1560	0.161
10.0	637	8.60	1.3510	0.1894	0.331
15.0	745	8.63	1.3589	0.2296	0.627
20.0	729	8.61	1.3665	0.2600	0.657

Table 5 : Effect of Salinity on IFT of TRS10-410/Dodecane system

Surfactant : 4% TRS10-410 Alcohol : 2% n-Butanol

Temperature : 90°C Oil : Dodecane

Salinity %NaCl	Drop Width x0.0001 cm	Spinning Rate(ms/rev)	Refractive Index	Δρ g/cc	IFT dynes/cm
0.6	384	8.49	1.3415	0.2470	0.099
0.8	362	8.50	1.3423	0.2518	0.0588
1	303	8.53	1.3429	0.2504	0.0488
1.2	244	8.53	1.3404	0.2412	0.0247
1.6	151	8.53	1.3378	0.2602	0.00634
2	132	8.55	1.3378	0.2586	0.00419
2.5	108	8.54	1.3388	0.2636	0.00234
3.0	107	8.55	1.3395	0.2706	0.00233
3.5	134	8.54	1.3404	0.2748	0.00464
4	254	8.49	1.3411	0.2722	0.0316
5	238	8.51	1.3426	0.2769	0.0263
5.5	310	8.52	1.3434	0.2872	0.0599
6.5	343	8.53	1.3453	0.2966	0.0833
7	353	8.53	1.3460	0.2922	0.0890
8	366	8.54	1.3475	0.2957	0.100
10	423	8.55	1.3444	0.2480	0.130
12	501	8.55	1.3537	0.2628	0.225
16	618	8.56	1.3605	0.2552	0.402
18	600	8.55	1.3635	0.2530	0.364
20	622	8.55	1.3665	0.2704	0.430

Table 6 : Effect of Salinity on IFT of Sapogenate T150/Crude Oil system

Surfactant : 4% Sapogenate T150 Alcohol : 2% n-Butanol

Temperature : 90°C Oil : Crude Oil

Salinity %NaCl	Drop Width x0.0001 cm	Spinning Rate(ms/rev)	Refractive Index	Δρ g/cc	IFT dynes/cm
1	341	8.56	1.3386	0.1287	0.0358
3	1014	8.56	1.3424	0.1656	0.062
5	834	8.55	1.3441	0.1796	0.724
8	1260	8.54	1.3510	0.2034	2.79
10	1792	8.57	1.3538	0.212	8.26
12	1587	8.56	1.3573	0.2380	6.40
14	1627	8.54	1.3600	0.2356	6.8
16	1844	8.56	1.3629	0.2332	9.72
18	1689	8.57	1.3663	0.2774	8.8

Table 9 : Surface Tension Data for CMC Determination

Surface tension of distilled water : 72.0 dyne/cm (mN/m)

Temperature : 26.7 °C

Surfactant Concentration g/l	Surface Tension, dyne/cm (mN/m)				
	V2880	V3348	B1083	B1139	T150
0.04	53.8	--	--	--	--
0.05	--	43.9	49.7	52.6	37.2
0.08	42.9	41.8	47.3	49.3	34.9
0.10	40.5	40.5	44.5	47.9	33.8
0.15	34.0	37.5	41.3	45.5	31.7
0.20	30.0	35.3	40.4	43.0	31.0
0.30	29.5	32.7	38.0	39.9	31.6
0.40	29.8	32.4	34.8	37.8	31.7
0.50	29.9	32.3	34.3	--	--
0.60	--	--	--	35.5	31.9
0.75	--	31.7	34.0	--	--
0.80	--	--	--	34.9	31.5
1.00	29.6	31.0	33.5	34.7	31.4
1.50	29.6	31.9	33.8	34.5	31.4
2.00	29.6	31.8	34.6	34.6	31.5
2.50	29.8	31.9	34.7	34.5	31.5
3.00	30.0	31.9	34.6	35.0	31.4
3.50	30.4	--	--	35.0	31.5
4.00	30.5	31.9	34.5	35.1	31.5
6.00	30.5	31.9	34.5	35.1	31.5

Table 10: Criticial Micelle Concentration Values

Temperature : 26.7 °C

Surfactant Name	Measured CMC g/l	Active Ingredient g/l	Active Ingredient Kmol/m^3
V2880	0.21	0.21/0.301=0.69	$0.69/720 = 9.6 \times 10^{-5}$
V3348	0.35	0.35/0.350=1.00	$1.00/808 = 1.2 \times 10^{-3}$
B1083	0.43	0.43/0.214=2.01	$2.01/1028 = 1.9 \times 10^{-4}$
B1139	0.69	0.69/0.259=2.66	$2.66/1168 = 2.3 \times 10^{-3}$
T150	0.17	0.17/1.0 =0.17	$0.17/1058 = 1.6 \times 10^{-4}$

Table 11a : Cloud Points of Various Surfactants

% NaCl Conc.	% Surf. Conc.	Cloud Point, °C V2380	B1083	T150
0	1	>100	>100	>100
0	2	>100	>100	>100
0	4	>100	>100	>100
1	1	>100	>100	>100
1	2	>100	>100	>100
1	4	>100	>100	>100
2.5	1	33.3	--	--
2.5	2	30.0	--	--
2.5	4	29.0	--	--
5	1	<25	--	--
5	2	<25	--	--
5	4	<25	--	--
10	1	<25	75.0	50
10	2	<25	74.0	48.5
10	4	<25	72.5	48.0
20	1	<25	47.0	33.5
20	2	<25	46.0	32.5
20	4	<25	45.0	31.5

Table 11b: Cloud Points of Various Surfactants in the Presence of n-Butanol

% NaCl Conc.	% n-Butanol Conc.	% Surf. Conc.	Cloud Point, °C V2880	B1083
1	1	4	>100	--
1	2	4	>100	--
1	4	4	>100	--
1	8	4	>100	--
2	1	4	>100	--
2	4	4	>100	--
2	8	4	35.0	--
5	1	4	<25	--
5	4	4	<25	--
5	8	4	<25	--
10	1	4	<25	--
10	4	4	<25	--
10	8	4	<25	--
20	1	4	--	35.0
20	4	4	--	<25
20	8	4	--	<25

Table 12 : Phase Inversion Temperature Studies

Surfactant :	4% V2880	Alcohol :	2% n-Butanol
Temperature :	Varied	Oil :	Crude Oil
Salinity :	20% NaCl		

Temp. °C	Drop Width x0.0001 cm	Spinning Rate(ms/rev)	Refractive Index	Δρ g/cc	IFT dynes/cm
26	221	8.46	1.3663	0.2676	0.0195
35	166	8.56	1.3659	0.2758	0.00845
45	227	8.53	1.3662	0.2638	0.0205
55	311	8.53	1.3660	0.2574	0.0515
75	343	8.56	1.3662	0.2738	0.0729
90	428	8.59	1.3654	0.2760	0.142

Table 13a : Effect of Salinity on IFT of V2880/Crude Oil System

Surfactant	: 4% V2880	Alcohol	: 2% n-Butanol
Temperature	: 90°C	Oil	: Crude Oil

Salinity %NaCl	Drop Width x0.0001 cm	Spinning Rate	Refractive Index	Δρ g/cc	IFT dynes/cm
3	742	8.56	1.4327	0.1400	0.398
4	689	8.57	1.3439	0.1444	0.327
5	620	8.55	1.3452	0.1420	0.235
6	557	8.57	1.3469	0.0994	0.117
7	289	8.57	1.4394	0.1754	0.0289
7.5	294	8.54	1.3495	0.1988	0.0348
8	286	8.56	1.3492	0.0842	0.0334
8.5	232	8.54	1.3507	0.2154	0.0184
9	233	8.55	1.3505	0.2184	0.0189
9.5	377	8.56	1.3501	0.2122	0.0777
10	497	8.54	1.3526	0.1740	0.146
12	321	8.56	1.3541	0.2140	0.0480
14	267	8.54	1.3572	0.2282	0.0294
15	163	8.53	1.3589	0.2591	0.00759
16	126	8.53	1.3604	0.2578	0.00339
17	343	8.58	1.3612	0.2642	0.0708
18	405	8.56	1.3634	0.2770	0.122
20	461	8.57	1.3657	0.2858	0.185

Table 13b: Partition Coefficients of V2880 with Crude Oil

Temperature : 90°C Alcohol : n-Butanol

Salinity Wt.%NaCl	Partition Coefficient
6	0.2
7	0.7
8	0.35
9	0.85
10	1.05
12	4.0
14	14.5
15	72.0

Table 14a : Effect of Salinity on IFT of V2880/Dodecane System

Surfactant : 4% V2880 Alcohol : 2% n-Butanol

Temperature : 90°C Oil : Dodecane

Salinity %NaCl	Drop Width x0.0001 cm	Spinning Rate(ms/rev)	Refractive Index	Δρ g/cc	IFT dynes/cm
4	614	8.58	1.3434	0.2658	0.4250
5	512	8.58	1.3443	0.2786	0.2580
6	390	8.58	1.3519	0.3004	0.1208
7	220	8.61	1.3570	0.3198	0.0227
8	106	8.59	1.3566	0.3386	0.0027
9	353	8.59	1.3494	0.3030	0.0907
10	336	8.60	1.3506	0.3084	0.0790
11	327	8.61	1.3464	0.3078	0.0734
12	245	8.57	1.3541	0.3372	0.0327
13	107	8.61	1.3544	0.3436	0.00282
14	93	8.57	1.3570	0.3496	0.00221
15	125	8.61	1.3587	0.3518	0.00445
15.5	130	8.63	1.3587	0.3618	0.00525
16	151	8.61	1.3601	0.3632	0.00827
16.5	222	8.63	1.3606	0.3530	0.0254
17	202	8.62	1.3626	0.3640	0.0237
18	213	8.62	1.3635	0.3814	0.0256
19	238	8.62	1.3641	0.3678	0.0324
20	286	8.60	1.3662	0.3772	0.0577

Table 14b Partition Coefficients of V2880 with Dodecane

Temperature : 90° C Alcohol : n-Butanol

Salinity Wt.%NaCl	Partition Coefficient
5	0.795
6	0.121
7	0.169
8	0.136
9	0.185
10	1.059
12	4.0
14	14.67
15	72.0
16	30.67
17	138
18	240
20	267

Table 15: Effect of Alcohol Concentration on IFT of V2880/Crude Oil System

Surfactant : 4% V2880 Alcohol : n-Butanol

Temperature : 90°C Oil : Crude Oil

Salinity : 20%

Alcohol Con. Wt %	Drop Width x0.0001 cm	Spinning Rate(ms/rev)	Refractive Index	$\Delta\rho$ g/cc	IFT dynes/cm
0.5	340	8.59	1.3666	0.2776	0.0715
1.0	379	8.58	1.3665	0.2668	0.0954
2.0	419	8.61	1.3670	0.2682	0.128
4.0	478	8.60	1.3688	0.2738	0.1945

Table 16a : Effect of Surfactant Concentration on IFT of B1083/Crude Oil System

Surfactant	: B1083	Alcohol	: n-Butanol
Temperature	: 90°C	Oil	: Crude Oil
Salinity	: 20%		

Surfactant Conc. Wt.%	Drop Width x0.0001 cm	Spinning Rate(ms/rev)	Refractive Index	Δρ g/cc	IFT dynes/cm
0.5	457	8.56	1.3581	0.2666	0.171
1.0	420	8.55	1.3654	0.2682	0.132
2.0	515	8.55	1.3669	0.2952	0.267
3.0	163	8.58	1.3663	0.2942	0.00835
4.0	53	8.55	1.3665	0.2712	0.00267
5.5	264	8.58	1.3672	0.2744	0.03318

Table 16b : Effect of Surfactant Concentration on IFT of V2880/Crude Oil System

Surfactant :	V2880	Alcohol :	n-Butanol
Temperature :	90°C	Oil :	Crude Oil
Salinity :	20%		

Surfactant Conc. Wt.%	Drop Width x0.0001 cm	Spinning Rate(ms/rev)	Refractive Index	Δρ g/cc	IFT dynes/cm
0.5	434	8.64	1.3595	0.2812	0.151
1.0	375	8.64	1.3637	0.2774	0.0953
2.0	280	8.64	1.3661	0.2822	0.0402
3.0	517	8.61	1.3590	0.2856	0.260
4.0	461	8.56	1.3657	0.2858	0.185
7.0	453	8.62	1.3671	0.3084	0.186

Table 17a : Effect of Salinity on IFT in B1083/Crude Oil System

Surfactant : 4% B1083 Alcohol : 2% n-Butanol

Temperature : 90°C Oil : Crude Oil

Salinity %NaCl	Drop Width x0.0001 cm	Spinning Rate(ms/rev)	Refractive Index	Δρ g/cc	IFT dynes/cm
4	855	8.61	1.3441	0.1674	0.707
5	786	8.62	1.3454	0.1756	0.581
6	749	8.63	1.4374	0.1856	0.528
7	651	8.6	1.3492	0.1916	0.327
8	575	8.63	1.3512	0.1801	0.246
9	533	8.6	1.3529	0.2202	0.203
10	523	8.66	1.3552	0.2156	0.184
12	480	8.67	1.3573	0.2214	0.151
13	425	8.67	1.3578	0.2384	0.120
14	392	8.61	1.3592	0.2484	0.0450
14.5	242	8.49	1.3584	0.2320	0.0225
15	265	8.52	1.3595	0.2354	0.0296
16	438	8.64	1.3617	0.2522	0.120
18	234	8.64	1.3646	0.2674	0.0214
20	53	8.55	1.3659	0.2856	0.00267
21	270	8.50	1.3679	0.2756	0.036
22	303	8.6	1.3679	0.2792	0.0506

Table 17b: Partition Coefficients of B1083 with Crude Oil

Temperature : 90°C Alcohol : n-Butanol

Salinity Wt.%NaCl	Partition Coefficient
5	0.156
6	0.159
7	0.33
8	0.60
9	0.27
10	0.29
12	0.33
13	0.22
14	0.22
16	1.68
18	1.1
20	12.2
22	22.7
24	4.6
25	4.32

Table 18a : Effect of Salinity on IFT of B1083/Dodecane System

Surfactant : 4% B1083 Alcohol : 2% n-Butanol

Temperature : 90°C Oil : Dodecane

Salinity %NaCl	Drop Width x0.0001 cm	Spinning Rate(ms/rev)	Refractive Index	Δρ g/cc	IFT dynes/cm
4	561	8.55	1.3455	0.2880	0.350
5	560	8.52	1.3449	0.2972	0.365
6	585	8.52	1.3466	0.2944	0.410
8	485	8.52	1.3490	0.3182	0.250
9	460	8.54	1.3508	0.3102	0.210
10	385	8.52	1.3519	0.3302	0.130
12	360	8.54	1.3558	0.3388	0.110
14	454	8.53	1.3586	0.3582	0.227
16	446	8.52	1.3618	0.3744	0.255
18	538	8.53	1.3655	0.3900	0.404
19	198	8.53	1.3669	0.4022	0.0206
20	163	8.47	1.3680	0.3990	0.0116
21	183	8.58	1.3691	0.4136	0.0165
22	133	8.47	1.3695	0.4100	0.00646
22.5	233	8.57	1.3710	0.3904	0.0374
23	287	8.48	1.3711	0.4166	0.161
23.5	307	8.55	1.3732	0.4306	0.0812
24	133	8.50	1.3723	0.4188	0.00667
25	128	8.50	1.3734	0.4252	0.00588
26	127	8.51	1.3752	0.4356	0.00584
30	175	8.53	1.3794	0.4550	0.0158

Table :18b Viscosity of Middle Phase Microemulsion of B1083 Dodecane System (salinity scan)

Surfactant : 4% B1083 Alcohol :2% n-Butanol

Temperature: 90°C Oil :Dodecane

Salinity % NaCl	Viscosity cp
8	31
10	8
12	1.9
14	3.5
16	48
19	25
20	20
21	12
23	11
24	11
26	12

Table 19a : Effect of Surfactant Concentration on IFT of B1083/Dodecane System

Surfactant : B1083 Alcohol : n-Butanol

Temperature : 90°C Oil : Dodecane

Salinity : 20%

Surfactant Conc. Wt.%	Drop Width x0.0001 cm	Spinning Rate(ms/rev)	Refractive Index	Δρ g/cc	IFT dynes/cm
1.0	532	8.41	1.3665	0.4024	0.414
2.0	519	8.38	1.3675	0.4062	0.390
3.0	402	8.41	1.3669	0.4144	0.183
4.0	125	8.52	1.3677	0.4276	0.00555
6.0	147	8.44	1.3688	0.4194	0.00899
8.0	127	8.44	1.3695	0.4080	0.00564
10.0	125	8.43	1.3715	0.4252	0.00558
15.0	115	8.52	1.3761	0.4374	0.00434
20.0	106	8.42	1.3776	0.4438	0.00351

Table :19b Viscosity of Middle Phase Microemulsion of B1083 Dodecane System

Surfactant : 4% B1083 Alcohol :2% n-Butanol

Temperature: 90°C Oil :Dodecane

Surfactant Conc. wt.%	Viscosity cp
1.0	---
2.0	3.644
3.0	5.466
4.0	9.11
6.0	10.932
8.0	11.843
10.0	15.5487
15.0	16.398
20.0	18.22

Table 20a: Effect of Alcohol Concentration on IFT of B1083/Crude Oil System

Surfactant :	4% B1083	Alcohol :	n-Butanol
Temperature :	90°C	Oil :	Crude Oil
Salinity :	20% NaCl		

Alcohol Conc. Wt.%	Drop Width x0.0001 cm	Spinning Rate(ms/rev)	Refractive Index	$\Delta\rho$ g/cc	IFT dynes/cm
0.5	204	8.54	1.3679	0.2810	0.0161
1.0	150	8.54	1.3671	0.2994	0.00669
2.0	120	8.54	1.3675	0.2958	0.00338
3.0	293	8.54	1.3679	0.2940	0.0488

Table 20b: Effect of Alcohol Concentration on IFT of B1083/Dodecane System

Surfactant	: 4% B1083	Alcohol	: n-Butanol
Temperature	: 90°C	Oil	: Dodecane
Salinity	: 20% NaCl		

Alcohol Conc. Wt.%	Drop Width x0.0001 cm	Spinning Rate(ms/rev)	Refractive Index	Δρ g/cc	IFT dynes/cm
0.5	553	8.49	1.3683	0.3952	0.446
1.0	481	8.51	1.3664	0.3810	0.283
2.0	223	8.52	1.3671	0.3952	0.0290
3.0	241	8.52	1.3705	0.4034	0.0373

Table 22 : Effect of Alcohol Chain length on IFT of B1083/Dodecane System

Surfactant :	4% B1083	Alcohol :	2%
Temperature :	90°C	Oil :	Dodecane
Salinity :	20% NaCl		

Alcohol Type	Drop Width x0.0001 cm	Spinning Rate(ms/rev)	Refractive Index	$\Delta\rho$ g/cc	IFT dynes/cm
Nil	547	8.53	1.3653	0.3922	0.428
Propanol	276	8.54	1.3668	0.4092	0.0570
Butanol	214	8.54	1.3678	0.4028	0.0261
Pentanol	153	8.55	1.3695	0.4068	0.00957
Hexanol	102	8.55	1.3661	0.4052	0.00285

Table 23 : Ternary Compositions for 12% Salinity

Surfactant : 4% B1083 Alcohol : 2% n-Butanol

Temperature : 90°C Oil : n-Dodecane

WOR	Surfactant Conc. (g/100 ml)			ME Composition (g)			ME Composition (%)		
	AQ	ME	OIL	AQ	SURF	OIL	AQ	SURF	OIL
1:2	1.05	15.7	0.004	1.96	0.35	0.174	79	14	7
1:1	0.93	14.03	0.004	2.28	0.295	0.111	85	11	4
2:1	0.59	19.44	0.005	2.28	0.389	0.296	72	13	10
4:1	0.32	30.0	0.012	1.231	0.360	0.133	71	20	9
6.5:1	0.59	26.7	0.011	2.274	0.534	0.163	76	18	6
9:1	1.25	27.5	0.014	2.286	0.55	0.141	77	18	5

* AQ =aqueous solution, ME =microemulsion, SURF = surfactant

Table 24 : Ternary Compositions for 20% Salinity

Surfactant : 4% B1083 Alcohol : 2% n-Butanol

Temperature : 90°C Oil : n-Dodecane

WOR	Surfactant Conc. (g/100 ml)			ME Composition (g)			ME Composition (%)		
	AQ	ME	OIL	AQ	SURF	OIL	AQ	SURF	OIL
1:2	1.32	70.5	0.004	0.769	0.846	0.444	37.5	41	21.5
1:1	0.111	94.4	0.019	0.242	0.472	0.333	23	45	32
2:1	0.027	92.8	0.097	0.171	0.371	0.296	20	44	36
4:1	0.045	88.9	0.197	0.205	0.444	0.355	20.4	44.2	35.4
6.5:1	0.043	91.7	0.412	0.336	0.550	0.311	28	46	26
9:1	0.03	90.0	3.01	0.231	0.54	0.437	19	45	36

* AQ =aqueous solution, ME =microemulsion, SURF = surfactant

Table 25 : Ternary Compositions for 24% Salinity

Surfactant : 4% B1083 Alcohol : 2% n-Butanol

Temperature : 90°C Oil : n-Dodecane

WOR	Surfactant Conc. (g/100 ml)			ME Composition (g)			ME Composition (%)		
	AQ	ME	OIL	AQ	SURF	OIL	AQ	SURF	OIL
1:2	0.059	34.7	0.004	0.199	0.218	0.444	27	25	53
1:1	0.048	44.86	0.012	0.128	0.224	0.259	12	35	42
2:1	0.050	45.47	0.006	0.171	0.182	0.296	26	28	46
4:1	0.051	40.0	0.014	0.091	0.20	0.43	13	28	59
6.5:1	0.141	43.09	0.008	0.222	0.292	0.395	25	32	43
9:1	0.022	46.9	3.11	0.231	0.281	0.288	29	35	36

* AQ =aqueous solution, ME =microemulsion, SURF = surfactant

Table 26 : Ternary Compositions for 20% Salinity

Surfactant : 4% B1083 Alcohol : 2% n-Butanol

Temperature : 90°C Oil : Crude Oil

WOR	Surfactant Conc. (g/100 ml)			ME Composition (g)			ME Composition (%)		
	AQ	ME	OIL	AQ	SURF	OIL	AQ	SURF	OIL
1:3	0.086	51.05	0.64	0.49	0.306	0.297	45	28	27
1:2	0.069	57.89	0.44	0.192	0.208	0.424	24	25	51
1:1	0.083	36.67	0.72	0.912	0.770	0.765	47	32	21
2:1	0.044	58.33	0.61	0.316	0.350	0.680	23	26	51
3:1	0.044	38.05	0.44	0.332	0.228	0.255	41	28	31
4:1	0.033	52.78	0.72	0.443	0.211	0.170	54	26	20
7:1	0.055	55.8	0.61	0.456	0.279	0.171	50	30	20
9:1	0.05	56.6	0.55	0.342	0.283	0.235	40	33	27

* AQ =aqueous solution, ME =microemulsion, SURF = surfactant

Table 27 : Ternary Compositions for High Surfactant Concentration at 20% Salinity

Surfactant : 20% Ξ1083 Alcohol : 10% n-Butanol

Temperature : 90°C Oil : Crude Oil

WOR	Surfactant Conc. (g/100 ml)			ME Composition (g)			ME Composition (%)		
	AQ	ME	OIL	AQ	SURF	OIL	AQ	SURF	OIL
1:4	0.53	57.5	0.003	0.06	0.23	0.085	15	62	23
1:2	0.41	65	0.005	0.091	0.39	0.085	16	69	15
1:1	0.25	72.5	0.012	0.119	0.87	0.17	10	75	15
2:1	0.17	73.3	0.14	0.175	1.43	0.17	10	80	10
4:1	0.092	74	0.006	0.344	1.71	0.102	16	79	5

* AQ =aqueous solution, ME =microemulsion, SURF = surfactant